Functions of Microtubules in the *Saccharomyces cerevisiae* Cell Cycle

Charles W. Jacobs,* Alison E. M. Adams,* Paul J. Szaniszlo,‡ and John R. Pringle*

*Department of Biology, The University of Michigan, Ann Arbor, Michigan 48109; and ‡Department of Microbiology and Center for Applied Microbiology, The University of Texas at Austin, Austin, Texas 78712

Abstract. We used the inhibitor nocodazole in conjunction with immunofluorescence and electron microscopy to investigate microtubule function in the yeast cell cycle. Under appropriate conditions, this drug produced a rapid and essentially complete disassembly of cytoplasmic and intranuclear microtubules, accompanied by a rapid and essentially complete block of cellular and nuclear division. These effects were similar to, but more profound than, the effects of the related drug methyl benzimidazole carbamate (MBC). In the nocodazole-treated cells, the selection of nonrandom budding sites, the formation of chitin rings and rings of 10-nm filaments at those sites, bud emergence, differential bud enlargement, and apical bud growth appeared to proceed normally, and the intracellular distribution of actin was not detectably perturbed. Thus, the cytoplasmic microtubules are apparently not essential for the establishment of cell polarity and the localization of cell-surface growth. In contrast, nocodazole profoundly affected the behavior of the nucleus. Although spindle-pole bodies (SPBs) could duplicate in the absence of microtubules, SPB separation was blocked. Moreover, complete spindles present at the beginning of drug treatment appeared to collapse, drawing the opposed SPBs and associated nuclear envelope close together. Nuclei did not migrate to the mother-bud necks in nocodazole-treated cells, although nuclei that had reached the necks before drug treatment remained there. Moreover, the double SPBs in arrested cells were often not oriented toward the budding sites, in contrast to the situation in normal cells. Thus, microtubules (cytoplasmic, intranuclear, or both) appear to be necessary for the migration and proper orientation of the nucleus, as well as for SPB separation, spindle function, and nuclear division.

THE budding yeast *Saccharomyces cerevisiae* offers an opportunity to study the mechanisms of cellular morphogenesis in an experimentally tractable eukaryotic system. In the course of the yeast cell cycle, a series of morphogenetic events results in the establishment of cell polarity, the appropriate positioning of organelles, and the localized incorporation of new cell-surface material. These events include the following (4, 7, 49, 50, 64). (*a*) Selection of a nonrandom budding site. Early in the cell cycle, a single bud emerges near a pole of the ellipsoidal cell; the choice of poles is determined by the mating type of the cell. (*b*) Organization of the budding site. Just before bud emergence, a small ring of chitin is formed in the largely nonchitinous cell wall; the bud then emerges within the confines of this chitin ring. At about the same time, there appears a ring of filaments of ~10 nm diameter, of unknown biochemical nature. These filaments encircle the mother-bud neck in close proximity to the plasma membrane; they remain in place as the bud grows, then disappear just before cytokinesis. (*c*) Differential growth of the bud. Expansion of the cell surface before bud emergence appears to be essentially isotropic. Subsequently, however, new cell-surface material is incorporated almost exclusively in the growing bud, while the mother cell remains essentially constant in size. (*d*) Apical growth of the bud. Although very small and very large buds may expand isotropically, the bud appears to grow predominantly by the incorporation of new cell-surface material at its tip. (*e*) Nuclear migration and orientation. Before nuclear division (during which the nuclear envelope remains intact), the nucleus migrates into the mother-bud neck and becomes oriented such that it extends into both mother cell and bud as it elongates. (*f*) Cytokinesis and septum formation. A chitin-containing septum is formed to separate mother and daughter cells; after division, the chitin ring and septum remain on the mother cell as a "bud scar".

As in other eukaryotic cells, these morphogenetic events seem likely to involve the action of various elements of the cytoskeleton, such as the actin (15, 41) and myosin (72) system. The actin is present as a complex set of cytoplasmic fibers and cortical spots, whose distributions change during the cell cycle in ways that suggest a role in the localized incorporation of new cell-surface material (1, 29). This suggestion is supported by the behavior of conditional actin mutants (41).

Yeast also contains apparently typical eukaryotic microtubules (4, 28, 36, 40, 47, 58). Electron microscopy and an-

Dr. Jacobs's present address is Department of Molecular Genetics, The Ohio State University, Columbus, Ohio 43210. Dr. Adams's present address is Department of Biology, Massachusetts Institute of Technology, Cambridge, Massachusetts 02139.

titubulin immunofluorescence have shown that these microtubules are present in both the nucleus and the cytoplasm throughout the cell cycle (4, 29) and that they apparently all emanate from one or the other face of the spindle-pole body (SPB)[1], a microtubule-organizing center embedded in the nuclear envelope (4, 30, 36). The single SPB of the unbudded, G1 cell duplicates at the beginning of the cell cycle (4, 49). The two SPBs then remain juxtaposed in the nuclear envelope and connected by a bridge structure (the "double SPB" configuration) as DNA replication occurs and the bud emerges and grows to a diameter ~0.4× that of the mother cell (6). The SPBs then separate rapidly as a short (~0.9 μm) spindle forms. The cytoplasmic face of the double SPB is consistently oriented toward the budding site, and the cytoplasmic microtubules extend toward (and generally into) the bud (4, 6, 29); this orientation is maintained by one of the SPBs (and associated cytoplasmic microtubules) after SPB separation (1, 29). The short spindle persists until the bud approaches the size of the mother cell and the nucleus migrates into the neck. The spindle then elongates rapidly to a final length of 6–8 μm (4, 6, 32, 36, 45), and spindle disassembly, nuclear division, and cell division quickly ensue.

The intranuclear microtubules are presumed to be involved in mitosis and nuclear division (4, 36, 45, 55), although the nature of this involvement is unclear (32). The roles of the cytoplasmic microtubules are still more problematic. The consistent association of the SPB and cytoplasmic microtubules with the budding sites in normal vegetative cells (see above), in normal and centrifugally perturbed zygotes (4), and in *cdc4* mutant cells (which produce multiple abnormal buds; 1, 5, 18) has suggested that these microtubules may be involved in the processes (such as localized activation of enzymes and the polarized movement of secretory vesicles) that allow the determination and organization of the budding site and the emergence and differential growth of the bud (1, 4, 6, 29). Such a role would be consistent with the evidence for involvement of microtubules in vesicle movement in other system (61, 71). However, it has also been clear that the spatial correlations noted above might instead reflect an involvement of the cytoplasmic microtubules in nuclear migration, spindle orientation, or spindle elongation.

Thus, to elucidate the actual functions of the yeast microtubules, it is necessary to specifically block microtubule assembly or function and assess the effects of such blockage on the events of interest. Such blockage might be achieved using either mutations (25, 40, 59, 66) or inhibitors. Previous studies of yeast using the inhibitor methyl benzimidazol-2-yl-carbamate (MBC) have provided some information. MBC blocked nuclear and cellular division (16, 53, 76) and caused chromosome loss when cells were blocked and then released (75), effects that could plausibly be attributed to an interference with intranuclear microtubule function. Indeed, genetic and biochemical studies have provided evidence for a direct interaction of MBC with yeast tubulin (28, 40, 66), and electron microscopy suggested that the drug caused microtubule disassembly in vivo (53, 76). The MBC-arrested cells mostly had large buds, suggesting that differential bud enlargement could continue in the absence of the cytoplasmic microtubules. However, the difficulty of visualizing these microtubules by electron microscopy (6, 36, 39, 53) made it uncertain how quickly and completely they were lost during drug treatment. Indeed, the large residual increase in cell number after addition of MBC to growing cultures (53, 76) suggested that this drug might be slow acting or incompletely effective. The observation that the related drug nocodazole (11, 22) was more effective than MBC both in inhibiting the assembly of *S. cerevisiae* tubulin in vitro (28) and in inhibiting division of the fungus *Wangiella dermatitidis* (27), together with the development of effective immunofluorescence procedures for yeast (1, 29), prompted us to examine the effect of nocodazole on *S. cerevisiae* cells. As this drug produced a rapid and apparently complete disassembly of the yeast microtubules, we then used it in a systematic investigation of the possible functions of these microtubules in the morphogenetic events of the cell cycle. Preliminary reports of portions of this work have been presented (26, 50).

1. *Abbreviations used in this paper*: ConA, concanavalin A; DAPI, 2,6-diamidino-phenylindole; MBC, methyl benzimidazol-2-yl-carbamate; SPB, spindle-pole body.

Materials and Methods

Reagents

Nocodazole (methyl-5-[2-thienylcarbonyl]-1-*H*-benzimidazole-2-yl-carbamate), Ficoll 400, and FITC-labeled rabbit antiserum to rat IgG were obtained from Sigma Chemical Co. (St. Louis, MO). FITC-labeled concanavalin A (FITC-ConA) and rhodamine-labeled ConA were obtained from E-Y Laboratories (San Mateo, CA) and fluorochrome-labeled phalloidins from Molecular Probes (Eugene, OR). Rat mAb to yeast tubulin (YOL1/34; reference 31) was a gift from John Kilmartin, Medical Research Council Laboratory of Molecular Biology (Cambridge, England), MBC (analytical standard grade) was a gift from DuPont Biochemicals (Wilmington, DE), and Calcofluor White M2R was a gift from American Cyanamid (Bound Brook, NJ).

Strains

Several *Saccharomyces cerevisiae* strains were used. The wild-type diploid C276 (*MATa/MATα*, prototrophic [73]) was used in most experiments. Other strains used were the haploids C276-4A (a *MATa* prototrophic segregant from C276) and A364A (*MATa adel ade2 ural his7 lys2 tyrl gall* [17]); the diploid CP1AB-1AA (*MATa/MATa*, prototrophic [1]); the tetraploid JPQP1 (*MATa/MATa/MATα/MATα*, prototrophic [1]); and the temperature-sensitive mutant diploids 314D5 (*MATa/MATα cdc4-1/cdc4-1 adel/adel ade2/ade2 ural/ural tyr1/tyr1* [18]) and 370.2.3D (*MATa/MATα cdc2-1/cdc2-1 leu1/leu1 ural/ural*, a spontaneous diploid derived from haploid strain 370.2.3 [references 8 and 9], obtained from C. Newlon, Dept. of Microbiology, UMDNJ–New Jersey Medical School, Newark, NJ). All strains were maintained as deep-frozen stocks (51).

Culture Conditions and Drug Treatments

Except as noted, all cultures were grown in the rich liquid medium YM-P (35), with or without additions as described below. Liquid cultures were incubated with rotary shaking at ~150 rpm, either at 36°C (for temperature-sensitive mutants incubated at their restrictive temperature) or 23–24°C (all other cultures). On the basis of the preliminary experiments described below, the following standard conditions were adopted for all experimental and control cultures described in Results. YM-P medium contained final concentrations of 1% (vol/vol) DMSO (control cultures) or 1% DMSO plus 15 μg/ml nocodazole or MBC[2] (experimental cultures). Nocodazole or MBC was added to the medium from a freshly prepared stock solution (3.3 mg/ml nocodazole or MBC in DMSO), together with sufficient additional DMSO to reach the final concentration of 1%.

2. We report the concentrations of the inhibitors in μg/ml because we were unable to obtain definitive information on their purity. Indeed, our observations suggest that different preparations of nocodazole might differ in this regard (see Discussion). On the assumption that the drug preparations were 100% pure, 15 μg/ml corresponds to ~50 μM for nocodazole and ~80 μM for MBC. For comparison, Quinlan et al. (53) reported using 100 μM MBC and Wood and Hartwell (76) used either 20 or 100 μg/ml MBC.

Except where noted, the experimental and control cultures were inoculated with cells from mid-exponential-phase, asynchronously dividing populations in YM-P medium. In some experiments, the inocula were populations that had been enriched for unbudded cells: cultures that had been grown in YM-P medium to late exponential or early stationary phase were centrifuged through 4–10% Ficoll density gradients, and the fractions containing suitably high proportions of unbudded cells were pooled to use as inocula.

Preliminary experiments with strain A364A indicated that in the absence of a solubilizing agent, adding up to 100 μg of nocodazole powder per milliliter of culture medium had no noticeable effect on exponentially growing cells. Likewise, adding up to 1% DMSO to the medium produced no apparent effect. However, when the medium contained 1% DMSO plus 10–20 μg/ml nocodazole (added as a solution in DMSO as described above), cell division was arrested for several hours before gradually resuming. At lower concentrations, nocodazole produced a much shorter or undetectable arrest of cell division. In addition, when nocodazole was added at ≥25 μg/ml to medium containing 1% DMSO, a precipitate formed and the arrest of cell division was brief or not detectable. Similar results were obtained in experiments with strain C276. Some experiment-to-experiment variability in the response of the cells to nocodazole was observed, as considered in the Discussion. In the experiments reported below, we were careful to determine directly that the nocodazole-induced arrest of cell proliferation and loss of cellular microtubules were in effect throughout the periods of interest.

The growth of individual cells was monitored by time-lapse photomicroscopy, essentially as described previously (19). Liquid YM-P medium containing DMSO or DMSO plus nocodazole was solidified by the addition of 0.3 g agar to 15 ml of medium. The medium was steamed for 3 min to dissolve the agar, poured into a plastic petri dish, and used within 12 h.

Measurement of Cellular Parameters

Cell numbers and cell morphologies were determined after fixation using a Coulter Counter and phase-contrast microscopy, as described previously (51); determinations of the proportions of budded and unbudded cells were based on counts of at least 300 cells in each sample. Nuclear positions and morphologies were determined using either Giemsa stain and bright-field optics (1, 19) or 2,6-diamidino-phenylindole (DAPI) and fluorescence microscopy (74). For quantitative assessment of nuclear positions, random fields of Giemsa-stained cells were photographed with the 35-mm camera attachment of a microscope equipped with a 100× objective and a 10× camera eyepiece. The negatives were projected and the positions of nuclei determined by measurements on the images of all cells with well defined nuclei. A reproducible reference point for these measurements was taken to be the point of intersection of the bud axis (a line drawn from the middle of the mother-bud neck through the apex of the bud) with the presumed smooth contour of the mother cell wall before bud emergence. The shortest distance from this point to any point on the nucleus and the maximum length of the mother cell as measured from this point were determined for each cell, and the ratio of these distances was defined as the "nuclear-migration index" for that cell. Use of this index helped to correct measurements of nucleus-to-neck distances for differences in the sizes of the mother cells. The indices determined ranged from 0 (for cells whose nuclei had migrated up to the reference point or extended past it into the mother-bud neck) to ~0.65 (see Fig. 5, and below). The nuclear-migration index was not defined for unbudded cells or for cells in which the nucleus had already divided.

Fluorescence Staining and Fluorescence Microscopy

Chitin rings were detected by staining cells with Calcofluor and observing them by fluorescence microscopy (65). Tubulin-containing structures were visualized by indirect immunofluorescence as described previously (1, 29), except that fixation was generally performed by addition of concentrated formaldehyde solution directly to the culture medium; the final concentration was 3.7% (wt/vol) formaldehyde. Except where noted, the cells were then recovered immediately by centrifugation and resuspended in phosphate-buffered formaldehyde (40 mM potassium phosphate [pH 6.5] containing 3.7% [wt/vol] formaldehyde). Cells were fixed in this solution for 0.5–12 h before preparation for immunofluorescence. Actin-containing structures were visualized using rhodamine- or FITC-conjugated phalloidin (1). The growth of bud tips was demonstrated by labeling cells with FITC–ConA as described in the legend to Table V. Fluorescence photomicrography was performed using a Leitz Orthoplan microscope as described previously (1).

Electron Microscopy

Serial-section electron microscopy was performed as described previously (1, 6).

Results

Rapid Blockage of Cellular and Nuclear Division by Nocodazole

When DMSO was added to an exponential-phase, asynchronously dividing population, the cells continued to proliferate exponentially and there was no change in the distribution of unbudded, small-budded, and large-budded cells (Figs. 1, *A* and *B*, and 2 *A*). In contrast, when nocodazole was added together with the DMSO, population increase ceased ~40 min after addition of the drug; cell numbers increased ~25% before arrest (Fig. 1 *A*). After arrest, cell numbers stayed constant for several hours. Population increase eventually resumed, but the actual duration of the arrest varied from experiment to experiment (see Discussion). After 2–3 h, the nocodazole-arrested populations consisted almost exclusively of large-budded cells (Figs. 1 *B*; 2 *B*), suggesting that bud emergence and differential bud enlargement could continue after cell division was arrested by nocodazole. This issue is addressed further below.

Nocodazole also blocked nuclear division. Staining with Giemsa revealed that although control cells exhibited a normal range of nuclear morphologies (Fig. 2 *C*), the nocodazole-arrested cells uniformly contained single, unelongated nuclei (Fig. 2 *D*). In one typical experiment, cells were fixed after 3 h of culture in medium containing DMSO or DMSO plus nocodazole. Of 520 budded cells examined in the control population, 78 contained two nuclei and 46 contained single nuclei elongated through the mother-bud necks. In contrast, of 500 budded cells examined in the nocodazole-arrested population, only five appeared to contain two nuclei and only two contained single nuclei elongated through the mother-bud necks.

In Giemsa-stained populations, it was not possible to distinguish between mother cells and buds in large-budded cells. Thus, it was not clear whether the nuclei in nocodazole-arrested cells were uniformly in the mother cells, uni-

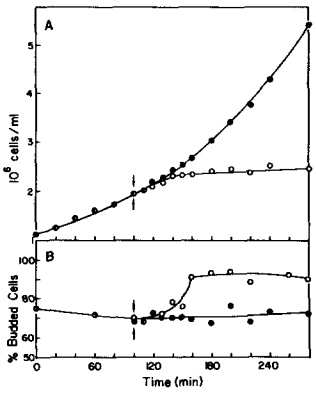

Figure 1. Cell numbers (*A*) and proportions of budded cells (*B*) in cultures of wild-type strain C276 grown in the presence (○) or absence (●) of nocodazole. Cells from a mid-exponential-phase culture were subcultured into fresh medium at $t = 0$. 100 min later, the culture was split (*arrows*); to one half was added DMSO and to the other half was added DMSO plus nocodazole, as described in Materials and Methods. At the indicated times, cell numbers and cell morphologies were determined. The data presented are averages from three independent experiments. For the purposes of this graph, doubly budded cells (see text) were simply scored as budded cells.

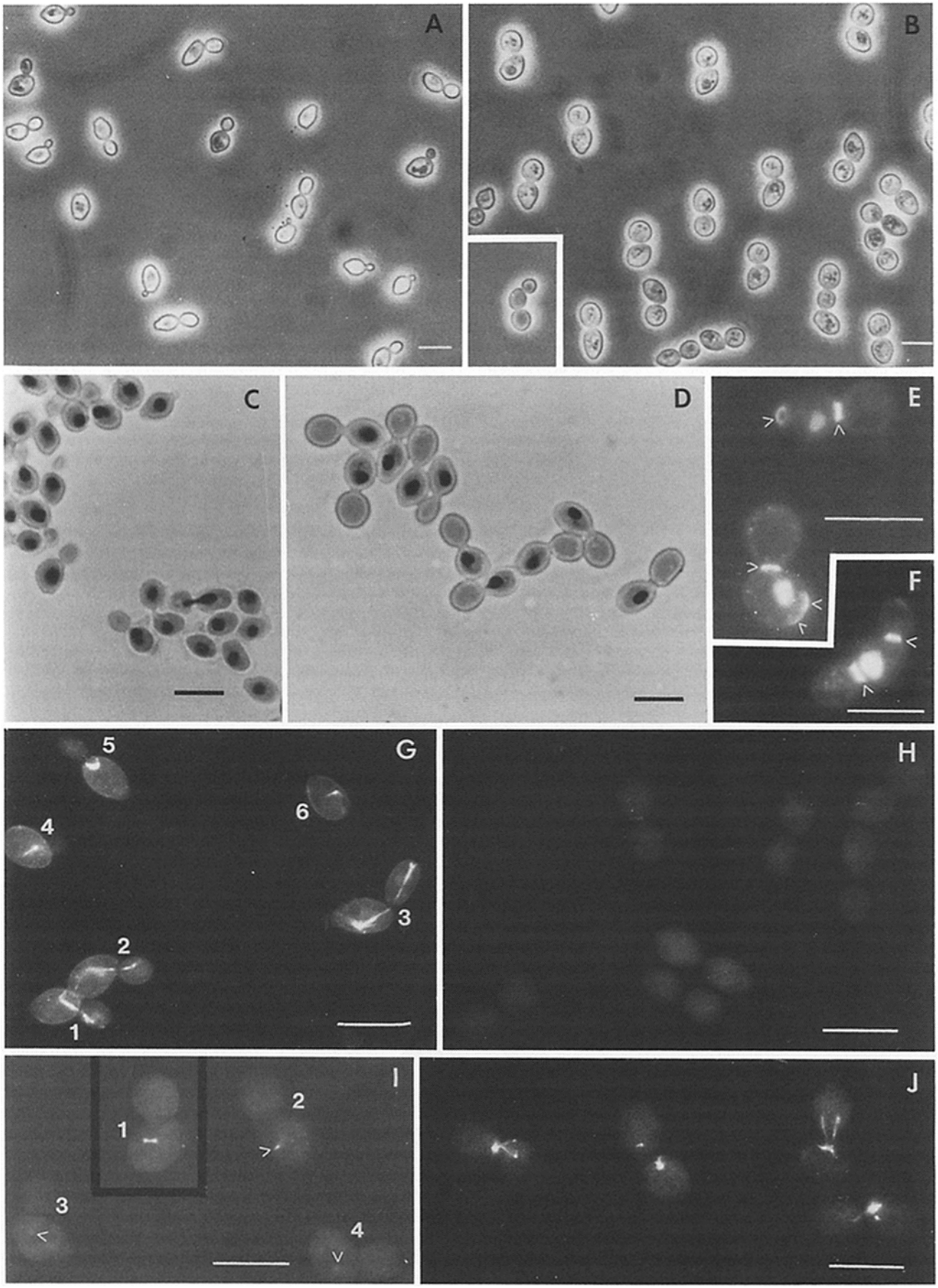
A
B
C
D
E
F
G
5
6
4
3
2
1
H
I
1
2
3
4
J

formly in the buds, or distributed between the two compartments. We addressed this problem by staining cells with both DAPI (to reveal nuclei) and Calcofluor (to reveal the bud scars on mother cells that had budded previously). In a population fixed after 3 h of incubation in nocodazole-containing medium, the nucleus was located in the mother cell in each of 300 budded cells on which at least one bud scar was seen (Fig. 2 *E*). The apparent effect of nocodazole on nuclear migration is addressed further below.

In arresting predominantly as large-budded, uninucleate cells, the nocodazole-treated populations resembled various cell-division-cycle (*cdc*) mutants in which specific steps in DNA replication or nuclear division appear to be blocked (49). However, the nocodazole-arrested populations were not completely homogeneous even at this level of analysis (see also below). In particular, ~5 to 10% of the mother cells appeared to have two buds (Fig. 2 *B*, *inset*). These cells appeared to have single nuclei located in the mother cells (Fig. 2 *F*), but we did not determine definitively whether both buds had cytoplasmic connections to the mother cells. Doubly budded cells were not observed in DMSO-treated control cultures.

Rapid Disassembly of Microtubules in Nocodazole-treated Cells

As nocodazole is known to interact with tubulins from *S. cerevisiae* and other organisms (10, 22, 28, 33, 42, 68, 70), we examined the effects of this drug on the yeast microtubule system. Immunofluorescence observations on cells from exponentially growing, DMSO-treated control cultures revealed tubulin-containing structures that were indistinguishable from those seen in normal cells; extended fluorescent arrays were detected in >95% of such cells (Fig. 2 *G*; Table I). In addition, the tubulin-containing arrays seen in cells that were fixed concurrently with exposure to nocodazole (by transferring cells into culture medium that contained formaldehyde as well as DMSO and nocodazole) were indistinguishable from those seen in control populations (data not shown). This was true even if the fixed cells were left in the nocodazole-containing medium for up to 60 min before recovery and processing for immunofluorescence. Moreover, the cells could be left in phosphate-buffered formaldehyde for periods of at least 12 h without any apparent effect on the immunofluorescence patterns subsequently observed. Thus, it appeared that DMSO alone did not affect the yeast microtubule system, that fixation by formaldehyde occurred rapidly, and that disassembly of microtubules in the fixed cells occurred slowly if at all, even in the presence of nocodazole.

In contrast, the tubulin-containing arrays appeared to diminish rapidly and progressively after exponentially growing cells were subcultured into nocodazole-containing medium (Table I). Extended structures resembling the original microtubule arrays were rarely detected after 30 min of exposure to the drug (Fig. 2 *I*) and almost never after 60 min of exposure (Fig. 2 *H*). Thus, it appeared that exposure of growing cells to nocodazole led to rapid disassembly of both intranuclear and cytoplasmic microtubules.

However, it seemed possible that the effect of nocodazole might be less drastic than suggested by the immunofluorescence observations. Thus, we also examined samples that were fixed with glutaraldehyde and prepared for electron microscopy. Cells from exponentially growing, DMSO-treated control populations contained apparently normal arrays of intranuclear and cytoplasmic microtubules (Fig. 3 *A*). Intranuclear microtubules were observed in essentially all cells in which SPBs were seen (data not shown), and cytoplasmic microtubules were observed in slightly more than half of such cells (Table II, experiment *1*). Essentially identical observations have been made on cells grown in medium without DMSO (6; our unpublished observations). The appearance of these microtubule arrays is consistent with the patterns of antitubulin immunofluorescence observed in such cells (e.g., Fig. 2 *G*; Table I; references 1, 29), except that immunofluorescence suggests that most or all cells contain cytoplasmic microtubules. This discrepancy presumably reflects the difficulty of visualizing these microtubules by electron microscopy (6, 36, 39, 53; Table II, ‡).

In contrast, the arrays of intranuclear and cytoplasmic microtubules were drastically diminished in nocodazole-treated cells (Fig. 3, *B–D*, *F*, and *H*; Table II, experiments *1* and *2*), consistent with the patterns of antitubulin immunofluorescence observed in such cells. The intranuclear microtubules seemed somewhat more persistent in the nocodazole-treated cells than were the cytoplasmic microtubules (Table II, §, ‖, and **), again consistent with the immunofluorescence observations (Table I, §).

In summary, the immunofluorescence and electron microscopic observations suggested that the inhibition of cellular and nuclear division by nocodazole might be a consequence of the rapid disassembly of microtubules.

Residual Tubulin-containing Structures in MBC-arrested Cells

MBC has also been shown to block cellular and nuclear division in *S. cerevisiae*, apparently by causing microtubule disassembly (see Introduction). However, it seemed desirable to reexamine MBC-arrested cells using antitubulin immunofluorescence. Addition of DMSO plus MBC to exponentially growing cells of strain C276 led to an arrest of division and the accumulation of large-budded cells within 3 h (data

Figure 2. Light micrographs illustrating morphological features of inhibitor-treated cells and of DMSO-treated control cells. Strain C276 was used. (*A–I*) Cells derived from experiments like those of Fig. 1. (*A–D*) Phase-contrast (*A* and *B*) and bright-field (*C* and *D*; Giemsa-stained cells) micrographs of cells fixed 3 h after addition of DMSO (*A* and *C*) or of DMSO plus nocodazole (*B* and *D*). The inset in *B* shows a doubly budded cell (see text). (*E* and *F*) Fluorescence micrographs of cells fixed 3 h after subculture into nocodazole-containing medium, then stained with both DAPI and Calcofluor. Arrows denote chitin rings; the small spots of fluorescence visible in some cells are due to DAPI staining of mitochondrial DNA (74). (*G–I*) Indirect antitubulin immunofluorescence micrographs of cells fixed after 60 min (*G* and *H*) or 30 min (*I*) of incubation in medium containing DMSO (*G*) or DMSO plus nocodazole (*H* and *I*). The numbered cells in *G* and *I* illustrate the types of tubulin-containing structures defined in Table I. (*J*) Indirect antitubulin immunofluorescence micrograph of cells fixed 3 h after addition of DMSO and MBC (see Materials and Methods) to an exponential-phase, asynchronously dividing population. Bars, 10 μm.

*Table I. Immunofluorescence Observations of Microtubule Disassembly During Treatment with Nocodazole**

Time of exposure to nocodazole	Percentage of cells displaying			
	Tubulin-containing arrays with ≥1 long element plus short elements	Tubulin-containing arrays without long elements but with short elements	One tubulin-containing bar or spot only	No detectable tubulin-containing structures
min				
0	60	36	4	0
Control‡	60–72	25–36	0–4	0–1
1	8	57	30	5
5	3	46	48	3
10	5§	21§	65	9
20	0	10§	68	22
30	0	3§	67	30
45	0	1§	50‖	48‖

* Cells from an exponential-phase culture of strain C276 were subcultured into medium containing DMSO or DMSO plus nocodazole. At intervals, samples were fixed and processed for antitubulin immunofluorescence as described in Materials and Methods, except that the phosphate-buffered formaldehyde contained 1% DMSO. For the initial (0 min) sample, cells were transferred into medium that already contained formaldehyde in addition to DMSO, and then processed as just described. The cells from all samples were scored for the presence of tubulin-containing structures including (*a*) "long elements" (fluorescent structures longer than half the length of the mother cell; e.g., cells 1–3 in Fig. 2 *G*); (*b*) "short elements" (asymmetric fluorescent structures of significant length, but less than half the length of the mother cell; e.g., cells 1–6 in Fig. 2 *G*. Cells 4–6 contain only short elements); (*c*) "bars" (isolated, symmetric fluorescent structures with well defined ends and length less than half that of the mother cell; e.g., cell 1 in Fig. 2 *I*); and (*d*) "spots" (point sources of fluorescence at the 1,000× magnification used; e.g., cells 2–4 in Fig. 2 *I*).

‡ The values obtained for the DMSO-treated control culture varied only slightly during the course of the experiment; the ranges observed for each category are indicated.

§ Most of the long and short elements observed in these samples appeared to be intranuclear based on their apparent location within DAPI-stained regions of the cells (cf. Table II, notes §, ‖, and **).

‖ In most experiments, >80% of the cells fixed after 45–60 min in nocodazole-containing medium contained no unequivocal tubulin-containing structures, and the remaining cells contained only fluorescent spots (e.g., Table II, note ‖). The particular experiment reported here was scored very conservatively (each point of fluorescence within the outline of a cell was scored as a "spot" even if it seemed likely to represent merely nonspecific background fluorescence); the results may also reflect the experiment-to-experiment variation in the response to nocodazole treatment (see Discussion).

not shown). About half of the arrested cells possessed extended, tubulin-containing structures even after a 3 h exposure to the inhibitor, although the structures observed (Fig. 2 *J*) were often very different from those seen in control cells (Fig. 2 *G*; reference 29). These results suggest that MBC may be less effective than nocodazole in producing disassembly of yeast microtubules (see Discussion).

Effects of Nocodazole on SPBs and Spindles

Electron microscopy also allowed a more detailed characterization of the cell-cycle block in nocodazole-arrested cells than was possible with light microscopy alone. In particular, it was possible to determine the behavior of the SPBs and the mitotic spindle. Examination of exponentially growing, DMSO-treated control cells revealed a normal distribution of SPB configurations (Fig. 3 *A*; Table III, experiment *I*). In contrast, when exponential-phase populations were treated with nocodazole, nearly all cells appeared to arrest with two SPBs in one or the other of two configurations. Most cells examined after 60 or 150 min of nocodazole treatment contained double SPBs (Fig. 3, *B* and *C*; Table III, experiment *I*). Except for the absence of microtubules, these double SPBs resembled those seen in cells with small buds during the normal cell cycle. However, in the cells treated with nocodazole for 150 min, the double SPBs were often located on deep invaginations of the nuclear envelope (Fig. 3 *C*), and the bridge structures sometimes appeared bent (Fig. 3 *C*) or broken (Fig. 3 *C*, *inset*; cf. Fig. 3 *B* and the normal double SPBs shown in reference 4). In most cells that did not contain double SPBs, the SPBs were distant from each other in the plane of the nuclear envelope, yet were opposed in close proximity (Fig. 3, *D–H*; Table III, experiment *I*). Each such SPB was located on a separate invagination of the nuclear envelope. The separation between such SPBs was typically ~0.2 μm (Fig. 3, *D–H*), in contrast to the ~0.95 μm of the normal short spindle (Fig. 3 *A*; references 4, 6, 39, 45). In most cases, no intranuclear microtubules were seen, but an unidentified fuzzy material was observed between the op-

Figure 3. Electron micrographs illustrating morphological features of nocodazole-treated and control cells. Cells of strain C276 were fixed at various times after subculture of exponentially growing populations into the appropriate media (Table II, experiment 1). (*A*) Control cell fixed after 60 min in DMSO-containing medium, illustrating the typical arrangement of SPBs (*arrows*) and intranuclear and cytoplasmic microtubules in a cell with a short spindle. The spindle in this particular cell is somewhat shorter than average (6, 39, 45; our unpublished observations). The bud is on the right; its cytoplasmic connection to the mother cell is out of the plane of section. (*B* and *C*) Cells fixed after 60 (*B*) or 150 (*C*) min in nocodazole-containing medium, illustrating double SPBs (*arrows*) without detectable intranuclear or cytoplasmic microtubules. In *C* and its inset (showing two different cells), the double SPBs are at the tips of deep invaginations of the nuclear envelopes on the sides opposite the buds, as revealed by examination of adjacent sections. (*D–H*) Cells fixed after 30 (*D*) or 60 (*E–H*) min in nocodazole-containing medium, illustrating closely opposed SPBs (*arrows*) without detectable intranuclear or cytoplasmic microtubules. Each SPB is located on a separate invagination of the nuclear envelope (*arrowheads* in *D*), as revealed by examination of adjacent sections. *E–G* show one cell in the first, third, and fifth sections from a series; *H* shows another cell. Bars: (*A–D*), 500 nm; (*E–H*, and *inset* in *C*) 250 nm.

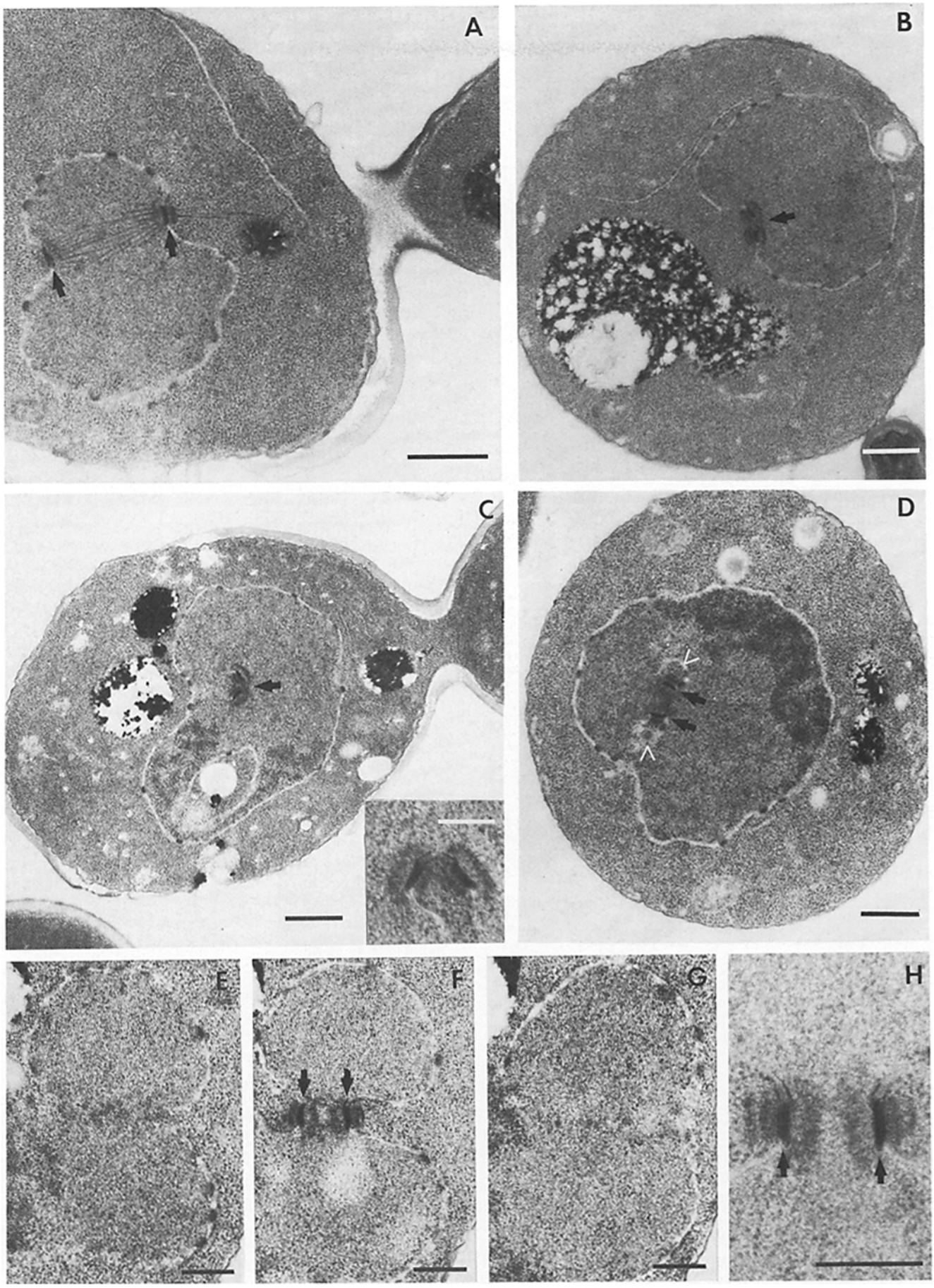
A
B
C
D
E
F
G
H

*Table II. Frequency of Detection of Cytoplasmic Microtubules by Electron Microscopy in Nocodazole-treated and Control Cells**

Experiment	Culture	Time of sampling	No. cells with detectable cMTs‡	No. cells without detectable cMTs‡
		min		
1	DMSO only	30	27	20
	DMSO only	60	26	23
	Nocodazole	30	2	36§
	Nocodazole	60	1	57‖
	Nocodazole	150	0	23¶
2	Nocodazole	60	1	19**
	Nocodazole	180	0	30‡‡

* In each experiment, samples were fixed and prepared for electron microscopy at the indicated times after inoculation of cells into medium containing DMSO or DMSO plus nocodazole. Samples were also taken at various times for determination of cell numbers, cell morphologies, and the status of microtubules as judged by immunofluorescence. For experiment *1* (actually a composite of data from two very similar experiments), the inocula were exponentially growing cells of strain C276. Cell proliferation continued unimpeded in the DMSO-treated culture and was arrested throughout the period of observation in the nocodazole-treated culture, essentially as in the experiments of Fig. 1. For experiment 2, the inoculum was a population enriched for small, unbudded cells (~91% of the cells were unbudded) from an early stationary-phase culture of strain JPQP1 (see Materials and Methods). Bud emergence began in both the nocodazole-treated and control cultures ~100 min after inoculation; by 180 min, ~50% of the cells in the nocodazole-treated population were budded. Cell numbers began to increase in the control culture by 170 min, but showed no increase even by 360 min in the nocodazole-treated culture, although >92% of the cells were budded.

‡ The presence or absence of cytoplasmic microtubules (cMTs) was scored by noting the SPBs that were identifiable in a set of serial sections. Each cell in which an SPB was found was then examined carefully for cytoplasmic microtubules both in the sections in which the SPB was visible and in several consecutive serial sections to either side of these. The detection of cytoplasmic microtubules was not always unambiguous, due to their small number and imperfect preservation, the presence of other cellular structures that resembled poorly preserved microtubules, and the variable angles of sectioning relative to the orientation of the microtubules. Each cell was tabulated according to the most plausible interpretation of the images. The presence or absence of intranuclear microtubules was also noted for most cells, but no rigorous quantitation was performed.

§ Immunofluorescence showed ~45% of the cells with no visible tubulin-containing structures, 48% with one bar or spot only, and 7% with one or more short elements (cf. Table I). Electron microscopy revealed short remnants of intranuclear microtubules on the face of the SPB in most cells, but microtubules of appreciable length were observed in only five of the 38 cells examined.

‖ Immunofluorescence showed ~88% of the cells with no visible tubulin-containing structures, 11% with one spot only, and 1% with a bar or short elements (cf. Table I). Electron microscopy revealed remnants of intranuclear microtubules (mostly as a short "stubble" on the face of the SPB) in about one third of the cells.

¶ Immunofluorescence showed ~84% of the cells with no visible tubulin-containing structure, 14% with one bar or spot only, and 2% with one or more short elements. Electron microscopy revealed unequivocal remnants of intranuclear microtubules in only one of the 23 cells examined.

**Immunofluorescence showed ≥75% of the cells with a single tubulin-containing spot and about 10% with a bar or short elements. (A problem with background fluorescence in this experiment made it difficult to get precise counts, particularly of the rather dim spots [cf. Fig. 2 *I*].) Electron microscopy revealed residual intranuclear microtubules of appreciable length (although much less extensive than in normal cells) in 19 of the 20 cells examined.

‡‡ Immunofluorescence showed ≥75% of the cells with no visible tubulin-containing structures, and <6% with structures more extensive than a single spot. (See comment in note **.) Electron microscopy revealed unequivocal remnants of intranuclear microtubules in only one of the 30 cells examined.

posed SPBs in favorable sections (Fig. 3 *D*, *F*, and *H*). Such opposed SPBs were never observed in control cells, but were seen in cells fixed after as little as 30 min of nocodazole treatment (Fig. 3 *D*).

Somewhat different results were obtained in related experiments in which populations consisting largely of small unbudded cells were inoculated into fresh medium containing nocodazole. In one such experiment (using strain JPQP1; Table III, experiment 2), nearly all cells examined 60 min after inoculation contained single SPBs (Fig. 4 *A*), as expected given that budding did not begin until ~40 min later (Table II, *). In these cells, cytoplasmic microtubules were essentially absent and intranuclear microtubules were drastically reduced (Table II). Nonetheless, cells examined 180 min after inoculation contained almost exclusively double SPBs (Table III). In a similar experiment (using strain C276), cells were fixed 240 min after inoculation into nocodazole-containing medium. This was ~150 min after budding (and presumably SPB duplication) had begun, and at least 180 min after extended tubulin-containing structures were last detected. Again, the arrested cells contained almost exclusively double SPBs (Fig. 4 *B*), although cells in a parallel sample from the DMSO-treated control culture contained mostly complete spindles or single SPBs. (The cells with single SPBs presumably had already divided once before fixation.) In both of these experiments, many of the double SPBs observed in the nocodazole-arrested cells were located on invaginations of the nuclear envelope (Fig. 4 *B*), and their bridge structures sometimes appeared bent or broken, as in the experiments using exponential-phase cells. However, closely opposed pairs of SPBs (Fig. 3, *D–H*) were seldom if ever observed in the experiments using inocula of small unbudded cells (Table III). The few cells in these experiments that did appear to contain either opposed SPBs or the remnants of complete spindles were probably derived from the few budded cells that had been present in the original inocula (see Table II, *).

Taken together, these results suggest that SPB duplication can occur in nocodazole-treated cells, but that SPB separation is then blocked. Thus, microtubules may be necessary for SPB separation but not for SPB duplication. In addition, the fact that closely opposed SPBs were observed only in arrested cells derived from asynchronously dividing populations suggests that these structures arose by the collapse of spindles that had been present in budded cells when the nocodazole-induced disassembly of microtubules began, as considered further in the Discussion.

Effects of Nocodazole on Nuclear Orientation and Nuclear Migration

The normal orientation of the double SPB toward the budding site was not perturbed by the addition of DMSO alone to the culture medium (data not shown). In contrast, the double SPBs observed in nocodazole-treated cells were often found in orientations inconsistent with the possibility that they were facing the bud sites and were sometimes oriented almost directly away from these sites (Figs. 3 *C* and 4 *B*). Most of these observations were made on arrested cells that were not strictly analogous to cells in normal populations because their buds had grown well beyond the point at which the SPBs normally separate. However, even when cells with small buds were examined specifically in appropriate samples, double SPBs oriented away from the bud sites were found frequently. For example, in a sample fixed 60 min after subculture of exponentially growing cells into nocodazole-containing medium (Tables II and III, experiment *I*), double SPBs were detected with reasonable confidence in 19 cells that had buds less than one third the diameters of the mother cells; in 11 cases, the double SPBs seemed to be

Table III. Configurations of SPBs in Nocodazole-treated and Control Cells

Experiment*	Culture	Time of sampling	Configuration of SPB‡				
			Single SPB	Double SPB	Complete spindle	Opposed SPBs	Ambiguous
		(min)					
1	DMSO only	60	17	15	32	0	9
	Nocodazole	60	4	49	9	22	16
	Nocodazole	150	0	12	1	6	4
2	Nocodazole	60	18	0	1	0	2
	Nocodazole	180	0	24	1	1?	4

* Experiments *1* and *2* are the same as those described in Table II.

‡ Individual nuclei were examined through sets of serial sections and categorized as containing one of the following configurations of SPBs (see Introduction for a description of the normal SPB cycle): (*a*) one single SPB (e.g., Fig. 4 *A*); (*b*) one double SPB (e.g., Figs. 3, *B* and *C*; 4, *B* and *C*); (*c*) a "complete spindle" (i.e., two single SPBs that were distant from each other in the plane of the nuclear envelope and separated by ≥0.7 μm on a direct line through the nucleoplasm [e.g., Fig. 3 *A*]; note that the "complete spindles" observed in nocodazole-treated cells contained at most remnants of the normal complement of spindle microtubules); or (*d*) "opposed SPBs" (i.e., two single SPBs that were distant from each other in the plane of the nuclear envelope but separated by <0.5 μm on a direct line through the nucleoplasm [e.g., Fig. 3, *D–H*]; see text for further discussion). The numbers tabulated should be regarded only as approximations, as the attempts to categorize nuclei in this way encountered nontrival difficulties. In particular, due to imperfect preservation, unfavorable angles of sectioning, or both, some putative SPBs were indistinct and difficult to distinguish unambiguously from similarly indistinct nuclear-pore complexes. Thus, it was not always possible to distinguish with confidence single from double SPBs, or a nucleus with one single SPB from a nucleus with two single SPBs at the poles of a "complete spindle". These problems were more acute in the nocodazole-treated cells than in the control cells (where the presence of microtubules helped to mark the bona fide SPBs), and were more acute in the diploid cells of experiment *1* than in the tetraploid cells of experiment *2* (where the greater discrepancy in size between SPBs and nuclear-pore complexes [see Fig. 4] helped to distinguish these structures). In all experiments, each nucleus was assigned to a category when such assignment could be made with even moderate confidence; the other nuclei examined were tabulated as "ambiguous".

oriented more than 90° away from the bud sites (e.g., Fig. 4, *C* and *D*).

In normal budded cells, undivided nuclei tend to be located close to the mother-bud necks and then migrate into the necks as spindle elongation begins. This behavior was not perturbed by DMSO. In populations growing exponentially in DMSO-containing medium, more than 95% of the budded, uninucleate cells had nuclear-migration indices (see Materials and Methods) of 0.25 or less and ~10% had nuclei actually extending through the mother-bud necks (Fig. 2 *C* and associated text; Fig. 5 *A*). In contrast, nocodazole-arrested cells appeared to have their nuclei positioned essentially randomly within the mother cells. In several populations fixed 3 h after subculture of exponentially growing cells into nocodazole-containing medium, only ~53% of the cells had nuclear-migration indices of 0.25 or less and <0.5% had nuclei extending through the mother-bud necks (Fig. 2 *D* and associated text; Fig. 5 *B*), although the buds on these cells had grown well beyond the size at which the nucleus normally migrates into the neck. Electron microscopic observations, though not performed quantitatively, suggested that the location of Giemsa-stained material was a generally accurate guide to the position of the nuclear envelope in nocodazole-arrested cells.

These observations suggested that nocodazole affected the positioning of the nucleus, but they were not entirely convincing because of the heterogeneity of nuclear position in the control populations (Figs. 2 *C* and 5 *A*). Thus, we investigated this problem further using a *cdc2* temperature-sensitive mutant strain in which most cells arrest at 36°C with large buds and with nuclei adjacent to the mother-bud necks (9). As expected, when this strain was incubated for 3 h at 36°C in DMSO-containing medium, most nuclei were very close to the necks (Figs. 5 *C* and 6 *A*); ~92% of the cells had nuclear-migration indices of 0.10 or less. In contrast, when the *cdc2* strain was incubated for 3 h at 36°C in nocodazole-containing medium, the nuclei appeared to be more randomly distributed within the cells (Figs. 5 *D* and 6 *B*); only ~14% of the cells had nuclear-migration indices of 0.10 or less.

A further question was whether nuclei that had already migrated to the mother-bud necks would remain there after microtubules were disassembled by nocodazole treatment. To address this question, *cdc2* cells were incubated for 3 h at 36°C to arrest the cells with their nuclei at the necks (cf. Figs. 5 *C* and 6 *A*). DMSO and nocodazole were then added, and the cells were incubated a further 2 h at 36°C. In each of two experiments, no extended tubulin-containing structures were observed by immunofluorescence in more than 200 cells examined after 60 min of exposure to nocodazole. In each experiment, ~81% of the cells had nuclear-migration indices of 0.15 or less before the addition of the drug. After 2 h of nocodazole treatment, the proportions were essentially the same (79 and 91%).

In summary, it appears that nocodazole interferes with the ability of the nucleus and SPB to orient toward, locate near, and migrate into the mother-bud neck, but does not disrupt the mechanisms that retain the post-migration nucleus in the neck region. Thus, microtubules are likely to be involved in the first three processes, but not in the last.

Bud Emergence and Bud Enlargement in Nocodazole-treated Cells

As described above, treatment of exponential-phase, asynchronously dividing cells with nocodazole yielded arrested populations that consisted almost exclusively of large-budded cells. The time course of events in these experiments suggested that both bud emergence and differential bud enlargement could occur normally in the absence of cytoplasmic microtubules. For example, in one of the experiments of Fig. 1, ~73% of the cells were budded after 30 min of nocodazole treatment, and the buds were of all sizes (as in Fig. 2 *A*). At this point, ≤10% of the cells appeared to contain appreciable remnants of their original microtubule arrays, mostly as intranuclear microtubules in cells that were

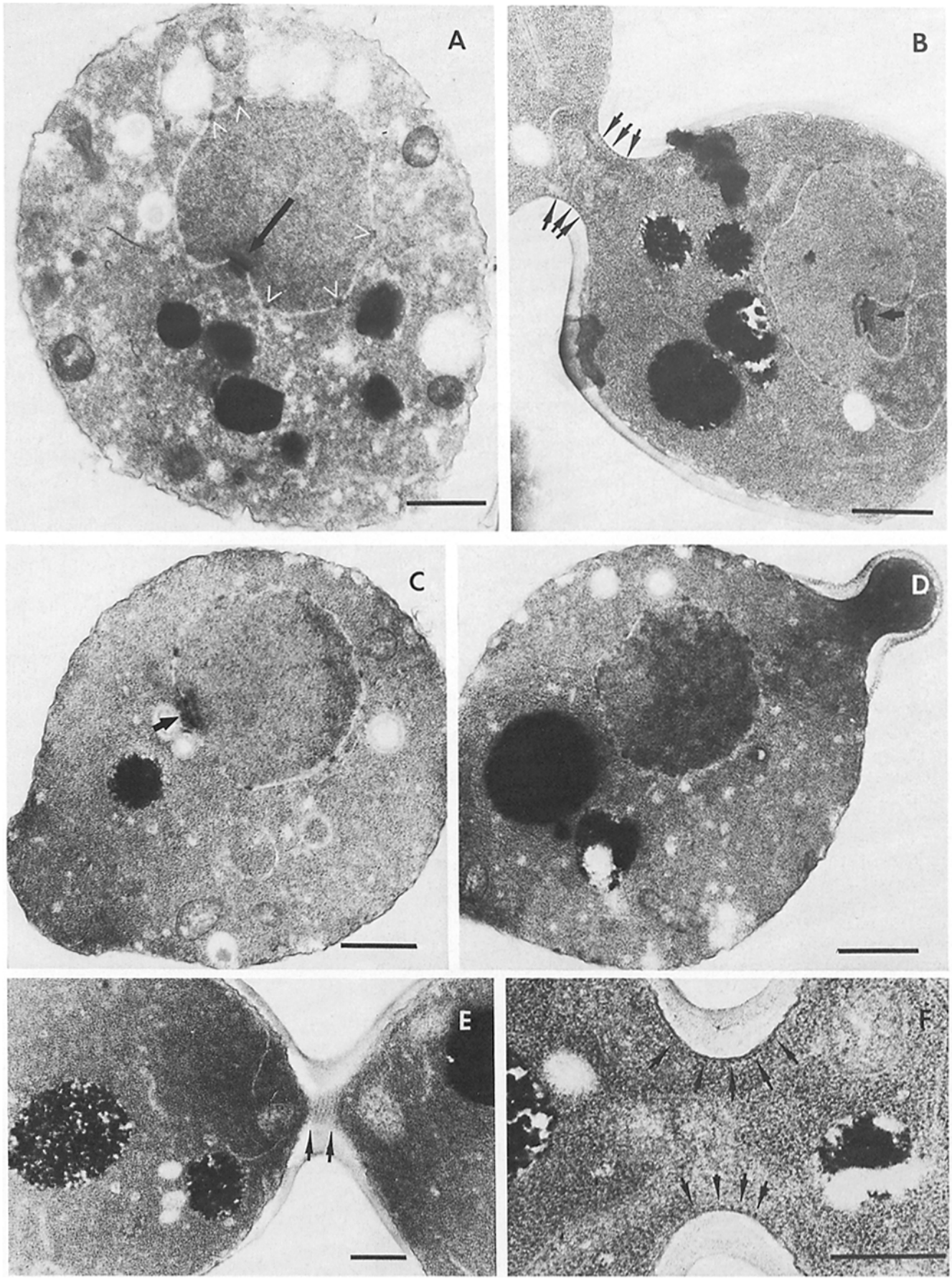
A
B
C
D
E
F

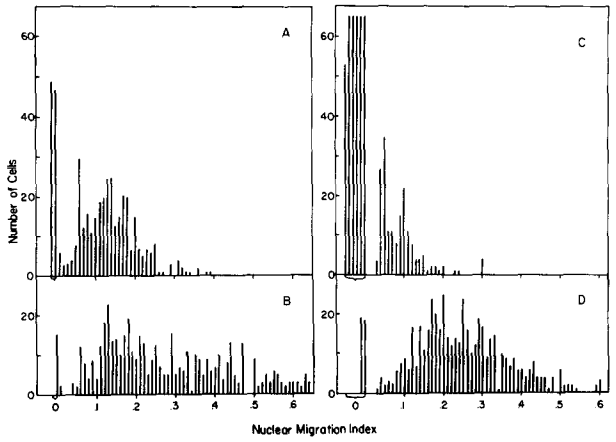

Figure 5. Histograms illustrating the effects of nocodazole on nuclear position in wild-type (*A* and *B*) and *cdc2* mutant (*C* and *D*) cells. The nuclear-migration indices of Giemsa-stained cells were determined as described in Materials and Methods; the smaller the index for a given cell, the closer was its nucleus to the mother-bud neck. The data presented in each panel are the cumulative results of several experiments of the same type. (*A* and *B*) Cells of strain C276 were examined after 3 h of incubation in medium containing DMSO (*A*) or DMSO plus nocodazole (*B*), in experiments like those of Fig. 1. *A* and *B* present data for 455 and 482 budded, uninucleate cells, respectively. (*C* and *D*) Cells of the temperature-sensitive strain 370.2.3D were examined after 3 h of incubation at 36°C in medium containing DMSO (*C*) or DMSO plus nocodazole (*D*). Essentially all cells in both populations were budded and uninucleate; *C* and *D* present data for 557 and 519 such cells, respectively. Immunofluorescence observations confirmed that the loss of microtubules was rapid and essentially complete in these experiments, as in the comparable experiments involving wild-type cells.

already budded (Figs. 2 *I* and 3 *D*; Tables I and II). During the subsequent 150 min, the fraction of cells with detectable tubulin-containing structures declined further and remained low (Figs. 2 *H* and *3*, *B* and *C*; Tables I, II). Nonetheless, during this period, the proportion of budded cells increased to >90% and essentially all buds approached or equalled their mother cells in size (Fig. 2, *B* and *H*).

Interpretation of these experiments was complicated somewhat by the large proportions of budded cells present initially and by the fact that tubulin-containing structures disappeared only gradually during the period in which bud emergence and bud enlargement were being monitored. Thus, we examined these processes also in experiments using inocula that had been enriched for unbudded cells. The results (Table IV) showed clearly that both bud emergence and differential bud enlargement could occur in the absence of detectable cytoplasmic microtubules. Very similar results were obtained in other experiments (Table II, experiment *2*; the experiment of Fig. 4 *B* and associated text) in which electron microscopy confirmed that microtubules were essentially absent during the period of interest.

To ask whether the selective expansion of bud tips could also occur in the absence of cytoplasmic microtubules, we used a procedure in which cells are first coated with FITC-ConA, then allowed to grow further in medium not containing added FITC-ConA. Foci of new cell-wall deposition then appear as nonfluorescent patches. To facilitate these experiments, we used a *cdc4* temperature-sensitive mutant strain that forms multiple, abnormally elongated buds when incubated at 36°C (18; Fig. 6, *C* and *D*). Most, if not all, of these buds contain cytoplasmic microtubules that reach essentially to their tips, and apical growth of the buds is easily demonstrated by the FITC-ConA procedure (1). When *cdc4* cells were incubated at 36°C to express the mutant phenotype, then incubated further at 36°C in the presence of nocodazole, they lost cytoplasmic microtubules as judged by immunofluorescence (Table V, 0-min samples). Nonetheless, the fraction of buds displaying well-defined apical growth during further incubation in the presence of nocodazole at 36°C was indistinguishable from that of a corresponding control culture (Fig. 6, *C–F*; Table V, 30-min samples). Thus, apical bud growth was apparently unimpeded by the loss of detectable cytoplasmic microtubules.

Formation of Chitin Rings and Rings of 10-nm Filaments in Nocodazole-treated Cells

Examination of exponentially growing populations that were treated with nocodazole suggested that both chitin rings and rings of 10-nm filaments could form in the absence of microtubules. For example, in the population illustrated in Fig. 2 *E*, chitin rings were observed at the bases of at least 308 of 314 buds examined, and in experiment 1 of Table II, 10-nm filaments were detected with reasonable confidence in 62 of 62 budded cells from the sample taken at 150 min (Fig. 4, *E* and *F*). However, interpretation of these observations was complicated somewhat by the facts (*a*) that many of the budded cells examined had already possessed buds (and thus, presumably, chitin rings and rings of 10-nm filaments) at the time of nocodazole addition and (*b*) that tubulin-containing structures disappeared only gradually after nocodazole addition. Thus, we also monitored formation of chitin rings and rings of 10-nm filaments in the experiments using inocula enriched for small, unbudded cells. As such cells are mostly daughter cells that have never budded, they are largely devoid of chitin rings and are presumably also devoid of rings of 10-nm filaments. Nonetheless, in experiment *A* of Table IV, chitin rings were observed on 98% of the cells

Figure 4. Electron micrographs illustrating morphological features of nocodazole-treated cells of strain JPQP1 (*A*) or C276 (*B–F*). (*A*) Representative cell fixed 60 min after inoculating a population of small unbudded cells into nocodazole-containing medium (Tables II and III, experiment 2), illustrating a single SPB (*arrow*) and nuclear-pore complexes (*arrowheads*). (*B*) Representative cell fixed 240 min after inoculating a population of small unbudded cells into nocodazole-containing medium (see text), illustrating a double SPB (*thick arrow*) lying in an invagination of the nuclear envelope. The 10-nm filaments in the neck region are also visible in cross section (*thin arrows*). (*C–F*) Cells fixed 60 (*C* and *D*) or 150 (*E* and *F*) min after subculture of an exponentially growing population into nocodazole-containing medium (Tables II and III, experiment 1). (*C* and *D*) The first and eighth sections from a series of a single cell, illustrating a double SPB (*arrow*) on the side of the nucleus opposite the bud. (*E* and *F*) Sections of two cells, illustrating tangential (*E*) and transverse (*F*) sections of the 10-nm filaments of the neck region (*arrows*). Bars, 500 nm.

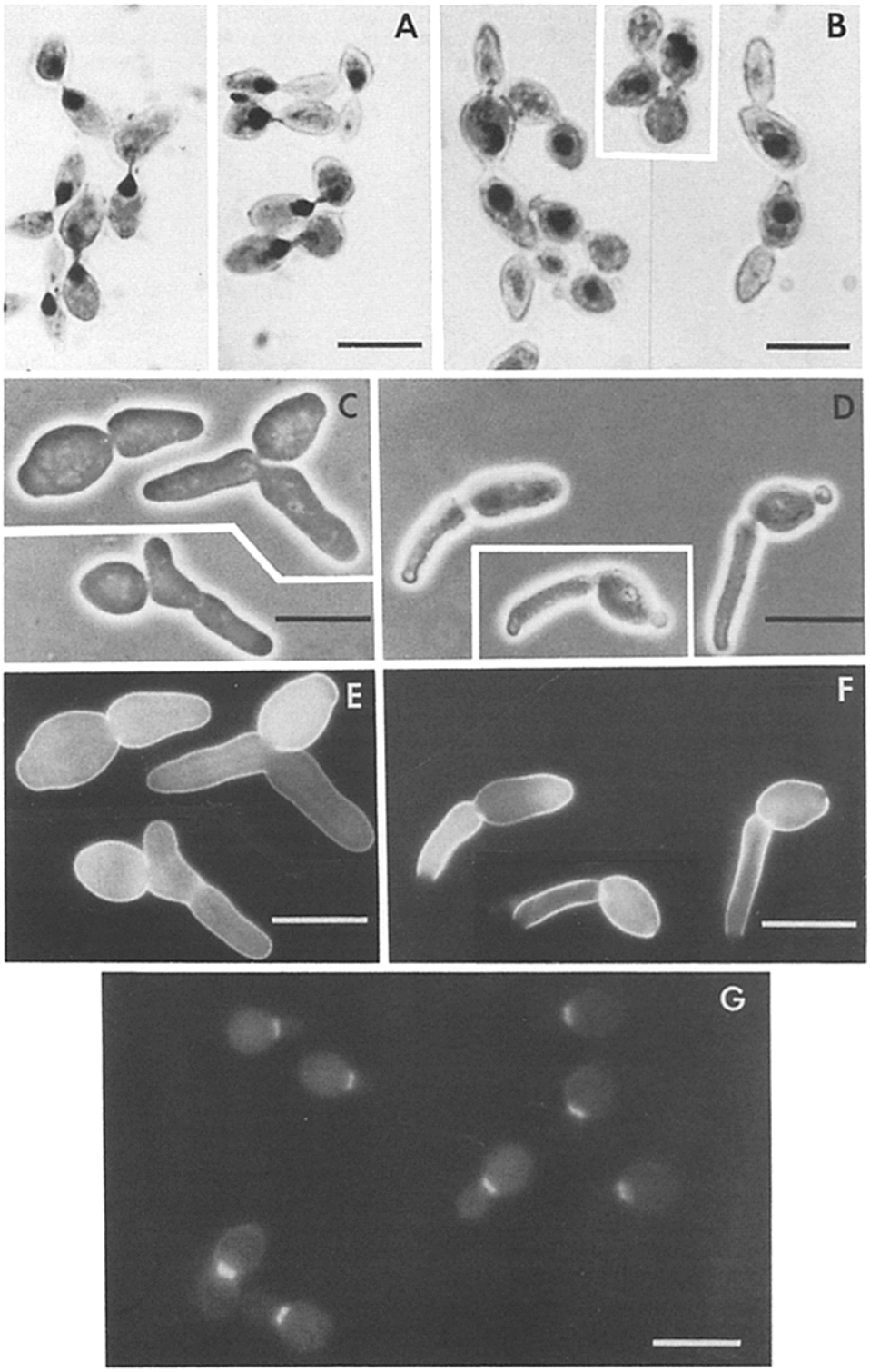

Figure 6. Light micrographs illustrating the effect of nocodazole on nuclear position in *cdc2* mutant cells (*A* and *B*), the failure of nocodazole to inhibit apical bud growth in *cdc4* mutant cells (*C–F*), and the failure of nocodazole to inhibit chitin-ring formation in wild-type cells (*G*). (*A* and *B*) Bright-field micrographs of Giemsa-stained cells of strain 370.2.3D after incubation in medium containing DMSO (*A*) or DMSO plus nocodazole (*B*), as described in the legend to Fig. 5. (*C–F*) Paired phase-contrast (*C* and *D*) and fluorescence (*E* and *F*) micrographs of nocodazole-treated *cdc4* cells immediately after staining with FITC–ConA (*C* and *E*) and after a further 30-min incubation in nocodazole-containing medium at restrictive temperature (*D* and *F*). These cells are from the experiment described in Table V. Each cell in *D* and *F* displays one or two FITC–ConA-dark foci. (*G*) Fluorescence micrograph of Calcofluor-stained cells from a sample fixed 240 min after inoculation of small, unbudded cells into nocodazole-containing medium (Table IV, experiment A). Bars, 10 μm.

in a sample taken at 240 min (Fig. 6 *G*; only 3% of the cells in the inoculum had chitin rings in this experiment), and in the experiment described in Fig. 4 *B* and the associated text, rings of 10-nm filaments were observed in 35 of 35 budded cells examined from the sample taken at 240 min (Fig. 4 *B*). Similar results (on both points) were obtained in experiment 2 of Table II. Given the data presented above on the time course of budding and loss of microtubules in these experiments, it seems clear that both chitin rings and rings of 10-nm filaments can form in the absence of microtubules.

It should also be noted that in these experiments, well defined rings of 10-nm filaments were observed in many cells that must have been arrested for considerable periods beyond the time at which these filaments would normally have disappeared (see Introduction). Thus, it seems that some event that is blocked by nocodazole (perhaps nuclear division) is

*Table IV. Bud Emergence and Differential Bud Enlargement in Nocodazole-treated Cells**

Experiment	Time of sampling	Percentage of budded cells	Percentage of cells displaying: Extended tubulin-containing structures‡	One tubulin-containing spot‡	No tubulin-containing structures
	min				
A	60	1	1	2	97
	180	69§	0	0	100
	300	98‖	0	0	100
B	0	25	ND	ND	ND
	60	60§	2	7	93
	180	98‖	0	1	99

* Medium containing DMSO plus nocodazole was inoculated with populations enriched for small, unbudded cells from early stationary-phase (experiment *A*) or late exponential-phase (experiment *B*) cultures of strain C276. At various times after inoculation, the proportions of budded cells and the types of tubulin-containing structures detectable by immunofluorescence were determined. Each percentage is based on a count of ~200 cells.
‡ These structures are defined and illustrated in Table I and Fig. 2, *G–I*. For present purposes, "extended tubulin-containing structures" include bars, short elements, and long elements. Note that both bars and spots seem generally to correspond to residua of intranuclear microtubules (Table I and II).
§ These budded cells exhibited a full range of bud sizes.
‖ About 90% of these budded cells had buds that approached or exceeded the mother cells in size.

a prerequisite for the disappearance of the ring of 10-nm filaments.

Selection of Budding Sites in Nocodazole-treated Cells

The results presented above suggested that the cytoplasmic microtubules are not involved in the organization of the budding site or in the emergence and enlargement of the bud. However, it remained possible that the microtubules are involved in selecting the nonrandom sites at which budding occurs. To address this issue, we used time-lapse photomicroscopy of cells incubated on solid medium containing DMSO or DMSO plus nocodazole. Given the results obtained with liquid cultures (Fig. 1), we expected that 25 to 30% of the nocodazole-treated cells would divide once, and that both mother and daughter cells would then bud again before arresting. Given the relatively long unbudded phases displayed by daughter cells (49), we expected that most daughter cells would bud again only at times at which the nocodazole-induced loss of microtubules would be essentially complete. Thus, we could ask whether the normal mating-type–specific positioning of the daughter cells' first buds was perturbed by this loss of microtubules. As shown in Table VI, which reports one of several very similar experiments, these expectations were realized. Moreover, it seemed clear from the results that neither DMSO nor DMSO plus nocodazole affected the normal positioning of the daughter cells' first buds in the *MATa/MATα* or *MATa/MATa* strains. A *MATa* haploid strain (C276-4A) behaved like the *MATa/MATa* diploid strain, although the films were more difficult to score because of the smaller, more rounded shape of the haploid cells. These results suggest that the cytoplasmic microtubules are not involved in the selection of budding sites, although an involvement in the positioning of the second and subsequent buds cannot be ruled out.

The Distribution of Actin in Nocodazole-treated Cells

As the cytoplasmic microtubules do not seem to be involved in the localized deposition of new cell wall, the burden of

*Table V. Apical Bud Growth in Nocodazole-treated and Control cdc4 Cells**

Culture	Time of sampling	Percentage of cells displaying ≥1 FITC-ConA-dark bud apex‡	Percentage of cells displaying: Extended tubulin-containing structures§	One tubulin-containing spot§	No tubulin-containing structures
	min				
DMSO only	0	0	98	2	0
DMSO only	30	75	97	2	1
Nocodazole	0	0	0	10	90
Nocodazole	30	71	0	12	88

* Cells of strain 314D5 growing exponentially at permissive temperature (23°C) were shifted to restrictive temperature (36°C) and incubated for 150 min. At this time, most cells displayed one or two abnormally elongated buds (see text and Fig. 6, *C* and *D*). The culture was then split; to one half was added DMSO and to the other half was added DMSO plus nocodazole. Incubation was then continued at 36°C for 60 min. One half of each culture was then stained with FITC-ConA and the other half with rhodamine-ConA, as described previously (1, 64, 67), except that the cells were incubated with the labeled lectins for 5 min at 36°C in buffers containing 1% DMSO or 1% DMSO plus 15 μg/ml nocodazole, as appropriate. The stained cells were then reinoculated into medium containing DMSO or DMSO plus nocodazole, as appropriate, and incubated further at 36°C. Immediately after reinoculation (time = 0) and 30 min later, a sample of each FITC-ConA-stained culture was fixed by addition of concentrated formaldehyde to a final concentration of 3.7% and used to observe staining of the cell wall (see text and Fig. 6, *C–F*), and a sample of each rhodamine-ConA-stained culture was processed for antitubulin immunofluorescence. (When FITC-ConA-stained cells were used for the antitubulin immunofluorescence, FITC fluorescence from residual cell wall obscured the staining of tubulin-containing structures by FITC-labeled antibodies.)
‡ Each percentage is based on a count of 200 cells; the remaining cells had only FITC-ConA-bright bud apices (for examples of dark and bright apices, see Fig. 6, *E* and *F*).
§ See Table IV, note ‡. Each percentage is based on a count of 200 cells.

*Table VI. Selection of Budding Sites in Nocodazole-treated and Control Cells**

Strain	Culture	No. cells examined	No. cells in which daughter cells budded‡	Position of daughter cell's first bud		
				Distal	Proximal	Ambiguous
C276	DMSO only	19	12§	9	1	2
	Nocodazole	47	13‖	11	0	2
CP1AB-1AA	DMSO only	19	18	0	17	1
	Nocodazole	49	13¶	0	11	2

* Exponentially growing cells of the *MATa/MATα* strain C276 and the *MATa/MATa* strain CP1AB-1AA were plated on medium containing DMSO or DMSO plus nocodazole and examined by time-lapse photomicroscopy as described in Materials and Methods. Except as noted, nearly all cells were followed for 5.5 to 6 h. For each cell that divided and proceeded to form new buds, we determined whether the daughter cell's new bud emerged near the pole distal or proximal to the point at which the daughter cell had been attached to its own mother cell. In some cases (scored as "ambiguous"), rotation of the cells, focus problems, or both, made it impossible to determine unambiguously where the new buds had emerged. Three lines of evidence indicated that microtubules were effectively disrupted in the nocodazole-treated cells throughout the period of observation. First, subsequent macroscopic inspection of the plates showed that growth of these cells had been grossly retarded relative to that of the cells exposed to DMSO alone. Second, immunofluorescence observations were performed on cells that were handled identically to those on which the time-lapse observations were made, except that they were washed off the plates and fixed after 1 or 3 h of incubation. For both strains at both time points, the DMSO-treated cells showed the expected arrays of tubulin-containing structures (cf. Fig. 2 *G*), whereas <10% of the nocodazole-treated cells showed any visible tubulin-containing structures (and these mostly just spots of fluorescence). Third, the time-lapse observations themselves showed that whereas essentially all cells in the DMSO-treated populations divided and proceeded at the expected pace into subsequent cell cycles, most cells in the nocodazole-treated populations appeared to arrest as large-budded cells.

‡ In nearly all of these cells, the mother cell had also produced a new bud by the time the daughter cell budded. In the nocodazole-treated populations, all of the cells that divided and proceeded to bud again had relatively large buds at the time of plating. Most of the new buds on daughter cells emerged betwen 1.25 and 3 h after plating. In each population, there were a few additional cells in which the mother cells appeared to bud again but the daughter cells did not. In the DMSO-treated populations, these were presumably just cases in which the daughters had not yet formed new buds when the observations were terminated. In the nocodazole-treated populations, these may also have been the "doubly budded cells" described above (Fig. 2, *B* and *F*, and associated text).

§ Observations were terminated by an accidental shift of the grid after ~3.5 h of incubation. At this time, some daughter cells (derived from cells that had originally been unbudded or had small buds) had not yet budded.

‖ Plus four cells in which only the original mother cell had produced a new bud when observations were terminated.

¶ Plus eight cells in which only the original mother cell had produced a new bud when observations were terminated.

suspicion falls more heavily on the actin-containing system, which has also been suggested to be involved in these processes (1, 29, 41). For this reason and to explore possible interactions among the cytoskeletal elements, it was important to ask whether the nocodazole-induced loss of microtubules perturbed the normal distribution of actin in the cells. As shown in Fig. 7, there was no evidence for such perturbation. Cells with small and large buds displayed asymmetric and relatively symmetric distributions of actin "dots", respectively, and the distribution of actin fibers was generally longitudinal, as in normal cells (1, 29, 41). A few large-budded cells displayed a concentration of actin in the neck region (Fig. 7 *B*), again as in normal cells. Finally, nocodazole-treated *cdc4* cells showed a dense clustering of actin "dots" at growing bud tips (not shown), as reported previously for *cdc4* cells not treated with nocodazole (1).

Discussion

Efficacy of Microtubule Inhibitors in Yeast

Disassembly of Microtubules and Inhibition of Cell Division by Nocodazole. Previous reports have shown that nocodazole interacts directly with yeast (28) and other (10, 22, 33, 42, 68, 70) tubulins, inhibits microtubule assembly in vitro (10, 28, 33), and produces microtubule disassembly in vivo (11, 56, 62). Our results showed that under the appropriate conditions, treatment of living yeast cells with nocodazole led to a rapid and essentially complete disassembly of both intranuclear and cytoplasmic microtubules, although the former appeared somewhat more persistent than the latter. These conclusions were based on observations by both electron microscopy and antitubulin immunofluorescence. However, we cannot altogether eliminate the possibility that a small population of microtubules persisted after drug treatment. The difficulty of visualizing the microtubules (particularly the cytoplasmic ones) by electron microscopy (6, 36, 39, 53; Table II) might have allowed such persistent microtubules to escape detection by this method, and we do not know the minimal number of microtubules necessary to yield a detectable immunofluorescence signal in this system. (It may be noted, however, that at least under favorable conditions, single microtubules can be detected by immunofluorescence [44].)

Treatment with nocodazole also produced a rapid and essentially complete inhibition of cell division; only ~25% of the cells in an exponentially growing population were able to divide after addition of the drug. The kinetics of arrest (Fig. 1) together with time-lapse observations (Table VI) made clear that the dividing cells had all been late in the cell cycle at the time of addition of the drug; that is, the cells displayed a distinct "execution point" (19, 48) for nocodazole at ~0.68 in the cell cycle. Effective disassembly of microtubules and inhibition of cell division in yeast by nocodazole have also been observed by others (20, 47).

Variable Efficacy of Nocodazole Treatment and Escape of Cells from Nocodazole Inhibition. The severity and duration of the nocodazole effects appear to be influenced by multiple factors, including at least one of the following. (*a*) The need for a solubilizing agent (see Materials and Methods). The 1% DMSO used here did not itself appear to affect either the microtubule arrays or the rate of cell division. (*b*) The surprisingly narrow range of concentrations at which nocodazole was effective. We observed little effect on cell division either at concentrations <10 μg/ml or when we tried to achieve concentrations ≥25 μg/ml (see Materials and Methods). (*c*) Sample-to-sample differences in the quality of nocodazole supplied by Sigma Chemical Co. We observed that different samples of nocodazole (even samples carrying the same lot number) could produce markedly different cellular responses at nominal concentrations of 15 μg/ml. (*d*)

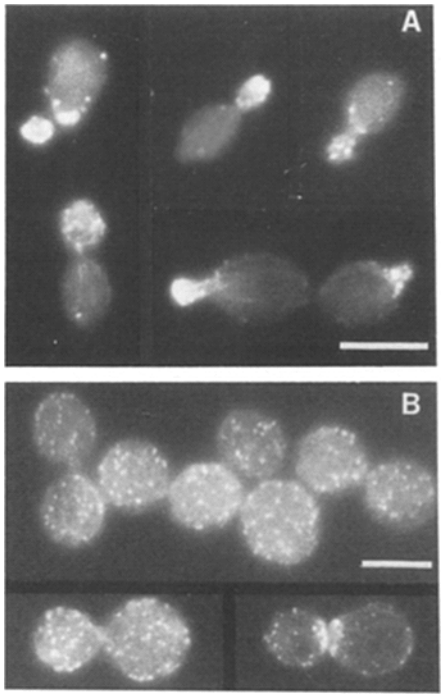

Figure 7. Fluorescence micrographs of FITC–phalloidin-stained cells, illustrating the distribution of actin in nocodazole-treated cells. Exponentially growing cells of strain C276 were shifted to medium containing DMSO plus nocodazole, and cells were examined after 1 h (*A*) or 3 h (*B*) of incubation. Parallel samples examined by antitubulin immunofluorescence revealed essentially no tubulin-containing structures in cells from either the 1- or 3-h sample. Bars, 10 μm.

Variations in response apparently depending on strain and growth conditions (47; our unpublished results).

Even under ostensibly optimal conditions, the inhibition produced by nocodazole was transient. In most of our experiments, we observed reappearance of microtubules, followed by resumption of cell division and new budding, beginning 5–9 h after the initial addition of nocodazole. A few cultures were arrested for even shorter periods and others remained arrested for as long as we followed the cultures (up to 12 h). Transient inhibition by nocodazole was also observed by Pillus and Solomon (47). The mechanism of escape from inhibition has not been investigated in detail, but may involve detoxification, as supplementation with fresh nocodazole appeared to prolong the period of inhibition (47). The transience and experiment-to-experiment variability of the nocodazole effects emphasize the importance of documenting directly that microtubules are indeed disassembled throughout the course of each experiment.

Relative Efficacies of Nocodazole and MBC. Most previous studies of yeast using microtubule inhibitors (12, 16, 40, 53, 59, 66, 75, 76) have used MBC or benomyl (which apparently breaks down to yield MBC as its microtubule-affecting stable product [16]). As noted above, the conclusions from these experiments about microtubule function were weakened by the uncertainty as to how effectively the microtubules had been disrupted by the drug. Indeed, our immunofluorescence observations showed that MBC-arrested cells could contain extensive (albeit apparently abnormal) tubulin-containing structures under conditions comparable to those in which nocodazole-treated cells contained essentially no such structures. Similar observations were made by Hašek et al. (20). The implication that nocodazole is more effective than MBC in disrupting yeast microtubule function is consistent with the observations (*a*) that nocodazole has a fourfold lower K_i than does MBC for inhibition of yeast tubulin assembly in vitro (28); and (*b*) that MBC-treated populations arrest division more slowly and show a nearly threefold greater increase in cell number before arrest than do nocodazole-treated populations (53, 76; Fig. 1 *A*; Jacobs, C. W., unpublished results). Nonetheless, most major conclusions drawn in the previous studies appear to be valid, based on comparison to the results obtained with nocodazole (this study), with tubulin mutants (25, 66), and with karyogamy-defective mutants (57). Apparent exceptions are the conclusions of Quinlan et al. (53) that SPB separation and nuclear migration could occur in cells without microtubules (see below). In addition, the conclusions about order-of-function derived from reciprocal-shift experiments using MBC and temperature-sensitive cell-cycle mutants (76) should be re-evaluated using nocodazole, as misleading results can be obtained in such experiments if either of the blocks used is slow-acting or incompletely effective (48).

Noninvolvement of Cytoplasmic Microtubules in the Establishment of Cell Polarity and Cell-Surface Morphogenesis in Yeast

Reproduction by budding involves the establishment of cell polarity and the subsequent localization of cell-surface growth. Presumably, the latter process depends on the localized delivery to the cell surface of vesicles carrying cell-surface precursors, enzymes, and enzyme-activating factors (4, 13, 52, 60). A variety of striking temporal and spatial correlations had suggested that the SPBs and cytoplasmic microtubules were involved in the establishment of cell polarity and the vesicle-delivery system in *S. cerevisiae* (1, 4–6). This hypothesis was consistent with the evidence for involvement of microtubules in polarized vesicle movement in animal cells (37, 54, 56, 61, 71), in the tip growth of hyphal fungi (23, 24), and in the determination of cell-wall shape in the fission yeast *Schizosaccharomyces pombe* (21, 69). However, our results with nocodazole-treated cells appear incompatible with this hypothesis—we could detect no effect of a loss of cytoplasmic microtubules on the selection of the budding site, the formation of the ring of 10-nm filaments and chitin ring at that site, or the emergence, differential enlargement, and apical growth of the bud. Cytokinesis and septum formation did not occur in the nocodazole-treated cells, but these effects were probably secondary to the blockage of nuclear division, as all other known inhibitors or mutations that block nuclear division in yeast also block cell division (25, 49). Similar results were obtained with tubulin mutants, which undergo bud emergence and bud enlargement and display no defect in invertase secretion or in the movement of mitochondria into the buds (25, 66). In addition, genetic and inhibitor studies with other fungi have also suggested that microtubules play no direct role in the growth of buds or hyphal tips (27, 43).

Our conclusions are subject to several caveats. First, as noted above, some microtubules might conceivably have escaped both disassembly and detection during nocodazole

treatment. Second, we do not know exactly when the cell commits itself to a new budding site, or exactly when the ring of 10-nm filaments forms. Thus, it is conceivable that these processes occurred before the cytoplasmic microtubules were fully disassembled in the relevant experiments. Third, the occurrence of second buds on some nocodazole-treated cells suggests that the loss of microtubules may in some way have perturbed the mechanisms that normally restrict a cell to one bud per nuclear cycle. Finally, it remains possible that the SPB is involved in the establishment of cell polarity or the organization of the budding site if it communicates with the cell surface by some non-microtubule means. However, the frequent misorientation of the double SPB in nocodazole-treated cells argues against this possibility.

If the SPB and cytoplasmic microtubules do not direct the polarization of growth in yeast, what does? The spatial and temporal associations of actin with regions of cell-surface growth (1, 29) and the behavior of actin mutants (41) strongly suggest that this protein is involved in the directed movement of secretory vesicles in yeast. This hypothesis also finds abundant precedents in other systems (3, 61, 63) and is consistent with our observation that nocodazole does not obviously perturb the actin distribution in budding cells. However, it is by no means clear whether the asymmetric distribution of actin establishes the cell polarity or is a consequence of an underlying polarity established by some unknown element. In this regard, the possible role of ion currents in the polarization of cell growth (3, 13, 14, 52) should not be overlooked. Studies of the basis for the mating-type–specific selection of budding sites may help to resolve these issues.

Involvement of Microtubules in the Nuclear Division Cycle

In contrast to its lack of effect on events at the cell surface, nocodazole had a profound effect on the behavior of the nucleus. Nuclear divison and apparently also nuclear elongation were blocked, presumably as a consequence of the disassembly of microtubules. As in any inhibitor experiment, such inferences are subject to the caveat that the inhibitor might have "side effects"; that is, nocodazole might block nuclear elongation or division by some means independent of its effect on the microtubules. However, this danger is minimized in the present case by (*a*) the extensive evidence from many systems that microtubules have a role in nuclear division, (*b*) the similar results obtained using MBC (16, 53, 76), and (*c*) the observations that tubulin mutations can either block nuclear division or confer altered sensitivity to the nuclear division blockage otherwise imposed by MBC (25, 40, 42, 66).

The microtubules essential for nuclear elongation and division presumably include the intranuclear microtubules (4, 25, 36, 45, 55), but may also include the cytoplasmic microtubules (2, 25, 32). A role for the latter would presumably have to be something more than their apparent involvement in nuclear migration (see below), as the behavior of *cdc24* mutants (which can undergo two rounds of nuclear division without budding; 49) indicates that nuclear migration is not a prerequisite for nuclear division. In this regard, it is of interest to consider also the implications of the closely opposed SPB configurations that were observed in some nocodazole-treated cells (Fig. 3; Table III; and associated text). Similar structures, but with the SPBs not so close together, were also observed in MBC-treated cells (53). Although our interpretation is tentative and requires verification (e.g., by examining the effects of nocodazole on synchronized populations), it appears that these structures arise by the collapse of short spindles present at the time of exposure to nocodazole. (From the nocodazole execution point [see above], the relationship between bud size and spindle length (6), and our electron microscopic observations (Table III), it appears that cells with longer spindles at the time of nocodazole exposure generally proceed to divide, although some may arrest with two well separated SPBs; the daughter cells resulting from such divisions, as well as cells that had single or double SPBs at the time of drug exposure, apparently arrest with unseparated double SPBs). If this interpretation is correct, then there must be an inward force acting on the SPBs, perhaps provided by the chromosomes (34) or by spindle matrix components (46). In normal cells, this force would be resisted by the intranuclear microtubules (34), the cytoplasmic microtubules (2, 32), or both. Interestingly, the inward force may not depend upon a tension developed between two separated SPBs, as double SPBs were also often found at the tips of deep invaginations of the nuclear envelope in nocodazole-treated cells. The bent or broken bridges found in these double SPBs may be a further indication of stressful forces. However, it is also possible that the presence of double SPBs on invaginations of the nuclear envelope reflected mechanisms different from those responsible for the formation of the "collapsed spindles". For example, continued growth of the nuclear envelope in the absence of guidance from microtubules might have resulted in folds or invaginations of the envelope. This view is consistent with the observation that the nuclear envelopes of nocodazole-treated cells often did appear very convoluted, with infoldings that contained single SPBs (in the cells exposed to nocodazole for 60 min) or no SPBs, in addition to those containing double SPBs. It may be relevant that *karl* mutants, which appear to have aberrant cytoplasmic microtubules, also display highly convoluted nuclear envelopes and SPBs at the tips of deep invaginations of these envelopes (57). It is also interesting that SPBs were observed at the tips of deep invaginations of the nuclear envelope during studies of normal cells by some (36, 39, 53, 55), but apparently not all (4–6, 32, 57), previous workers; conceivably, the resultant of the inward and outward forces acting on the SPB may vary from yeast strain to yeast strain, be affected by the precise conditions during fixation, or both.

The SPBs observed in nocodazole-treated cells appeared at least grossly normal in structure, in contrast to the report by Quinlan et al. (53) that the SPBs in MBC-treated cells lacked the outer (cytoplasmic) component. Thus, it appears that SPB structure can be maintained in the absence of microtubules or other tubulin detectable by immunofluorescence. In addition, our data on SPB configurations suggest strongly that SPB duplication is microtubule independent but that SPB separation depends on the intranuclear microtubules, the cytoplasmic microtubules, or both. Both conclusions are weakened somewhat by the difficulties in scoring SPB configurations reliably (see Table III, ‡), and the former conclusion is subject to the caveat that some remnant microtubules might have been present when SPB duplication occurred. The latter conclusion is subject to the caveat that nocodazole might have non-microtubule-mediated effects,

and needs confirmation using the tubulin mutants. In addition, our conclusion conflicts with that of previous workers (45, 53) that SPB separation is microtubule independent. However, Quinlan et al. (53) worked with the apparently less effective drug MBC, whereas Peterson and Ris (45) reasoned from morphological considerations that overlooked some possible modes of microtubule involvement in the process.

Our data also suggest strongly that microtubules (presumably cytoplasmic) are involved in the orientation of the SPBs (and thus ultimately of the spindle) and in the migration of the nucleus into the neck. As noted previously (1, 29), these hypotheses provide alternative explanations for the morphological correlations that had originally suggested microtubule involvement in secretory vesicle movement, and they imply that the microtubules must interact (directly or indirectly) with whatever system is responsible for the establishment of cell polarity. A role for the cytoplasmic microtubules in nuclear migration is strongly supported by observations on vegetatively growing tubulin mutants (25), as well as by the observations that microtubule abnormalities produced by drugs (12) or mutations (25, 57) interfere with nuclear migration and fusion, but not with cell fusion, during mating. Microtubules also appear to be involved in nuclear migration or positioning in fission yeast (68, 69, 70), *Aspergillus* (42, 43), and at least some plants (38). The orientation of SPBs has not yet been examined in the tubulin mutants, so it remains possible that the misorientation in nocodazole-treated cells is a non-microtubule-mediated effect of the drug.

Our conclusions that microtubules are essential for nuclear migration and elongation differ from previous conclusions that non-microtubule forces must be responsible for these processes (4, 6, 32, 36, 55). The previous conclusions were based on electron micrographs showing that the spindle frequently does not lie along the long axis of the nucleus as the latter begins to elongate through the mother-bud neck. We are not certain how to resolve this paradox, but the following considerations are relevant. First, it is conceivable that the discrepancy is only apparent; more systematic electron microscopic observations of nocodazole-treated cells might reveal movements of the nuclear envelope that are not detectable using DNA-specific stains and light microscopy. Second, our own observations of convoluted nuclear envelopes (see above) and of the failure of *cdc2* nuclei to leave the necks after microtubule disassembly (see Results) also provide some evidence for non-microtubule forces acting on the nuclear envelope. Third, it is possible that the ability of the putative non-microtubule forces to produce migration or elongation of the nuclear envelope might depend on the presence of the microtubules or on the prior occurrence of some microtubule-dependent event. A plausible model, consistent with all of the available data, is that the cytoplasmic microtubules are responsible for the migration of the nucleus to the neck and for the spindle orientation that results in one SPB's being in the mother cell and one in the bud. Non-microtubule forces would then be responsible for anchoring the nucleus at the neck and for the early stages of nuclear elongation through the neck. The final stages of nuclear elongation, in which the spindle does define the long axis of the nucleus (4, 6, 32, 36, 55), would then again be dependent on microtubules (intranuclear, cytoplasmic, or both).

We thank David Botstein, Tim Huffaker, Jim Thomas, and other members of their group for cordial and generous communication of unpublished information and helpful discussions; John Kilmartin for the gift of antibody; Lee Hartwell, Carol Newlon, and Charlotte Paquin for yeast strains; Breck Byers, Loretta Goetsch, and C. F. Robinow for instruction in microscopy techniques; and Susan Brown, Breck Byers, Keith Gull, Lee Hartwell, Jeremy Hyams, John Kilmartin, Dick McIntosh, Lorraine Pillus, C F. Robinow, Mark Rose, Randy Schekman, and Frank Solomon for helpful discussions.

This work was supported by National Institutes of Health (NIH) grant GM-31006 (J. R. Pringle), NIH postdoctoral fellowship GM-09727 (C. W. Jacobs), and the Biomedical Research Support grant to The University of Michigan from the NIH.

Received for publication 17 March 1988, and in revised form 27 May 1988.

References

1. Adams, A. E. M., and J. R. Pringle. 1984. Relationship of actin and tubulin distribution to bud growth in wild-type and morphogenetic-mutant *Saccharomyces cerevisiae*. *J. Cell Biol.* 98:934–945.
2. Aist, J. R., and M. W. Berns. 1981. Mechanics of chromosome separation during mitosis in *Fusarium* (Fungi imperfecti): new evidence from ultrastructural and laser microbeam experiments. *J. Cell Biol.* 91:446–458.
3. Brawley, S. H., and K. R. Robinson. 1985. Cytochalasin treatment disrupts the endogenous currents associated with cell polarization in fucoid zygotes: studies of the role of F-actin in embryogenesis. *J. Cell Biol.* 100:1173–1184.
4. Byers, B. 1981. Cytology of the yeast life cycle. *In* The Molecular Biology of the Yeast *Saccharomyces*: Life Cycle and Inheritance. J. N. Strathern, E. W. Jones, and J. R. Broach, editors. Cold Spring Harbor Laboratory, Cold Spring Harbor, New York. 59–96.
5. Byers, B., and L. Goetsch. 1974. Duplication of spindle plaques and integration of the yeast cell cycle. *Cold Spring Harbor Symp. Quant. Biol.* 38:123–131.
6. Byers, B., and L. Goetsch. 1975. Behavior of spindles and spindle plaques in the cell cycle and conjugation of *Saccharomyces cerevisiae*. *J. Bacteriol.* 124:511–523.
7. Cabib, E., R. Roberts, and B. Bowers. 1982. Synthesis of the yeast cell wall and its regulation. *Annu. Rev. Biochem.* 51:763–793.
8. Conrad, M. N., and C. S. Newlon. 1983. *Saccharomyces cerevisiae cdc2* mutants fail to replicate approximately one-third of their nuclear genome. *Mol. Cell. Biol.* 3:1000–1012.
9. Culotti, J., and L. H. Hartwell. 1971. Genetic control of the cell division cycle in yeast. III. Seven genes controlling nuclear division. *Exp. Cell Res.* 67:389–401.
10. Davidse, L. C., and W. Flach. 1977. Differential binding of methyl benzimidazol-2-yl carbamate to fungal tubulin as a mechanism of resistance to this antibiotic agent in mutant strains of *Aspergillus nidulans*. *J. Cell Biol.* 72:174–193.
11. De Brabander, M. J., R. M. L. Van de Veire, F. E. M. Aerts, M. Borgers, and P. A. J. Janssen. 1976. The effects of methyl [5-(2-thienylcarbonyl)-1H-benzimidazol-2-yl]carbamate, (R 17934; NSC 238159), a new synthetic antitumoral drug interfering with microtubules, on mammalian cells cultured *in vitro*. *Cancer Res.* 36:905–916.
12. Delgado, M. A., and J. Conde. 1984. Benomyl prevents nuclear fusion in *Saccharomyces cerevisiae*. *Mol. Gen. Genet.* 193:188–189.
13. Gooday, G. W. 1983. The hyphal tip. *In* Fungal Differentiation: A Contemporary Synthesis. J. E. Smith, editor. Marcel Dekker, New York. 315–356.
14. Gow, N. A. R. 1984. Transhyphal electrical currents in fungi. *J. Gen. Microbiol.* 130:3313–3318.
15. Greer, C., and R. Schekman. 1982. Actin from *Saccharomyces cerevisiae*. *Mol. Cell. Biol.* 2:1270–1278.
16. Hammerschlag, R. S., and H. D. Sisler. 1973. Benomyl and methyl-2-benzimidazole-carbamate (MBC): biochemical, cytological and chemical aspects of toxicity to *Ustilago maydis* and *Saccharomyces cerevisiae*. *Pest. Biochem. Physiol.* 3:42–54.
17. Hartwell, L. H. 1967. Macromolecule synthesis in temperature-sensitive mutants of yeast. *J. Bacteriol.* 93:1662–1670.
18. Hartwell, L. H. 1971. Genetic control of the cell division cycle in yeast. II. Genes controlling DNA replication and its initiation. *J. Mol. Biol.* 59:183–194.
19. Hartwell, L. H., J. Culotti, and B. Reid. 1970. Genetic control of the cell division cycle in yeast, I. Detection of mutants. *Proc. Natl. Acad. Sci. USA.* 66:352–359.
20. Hašek, J., J. Svobodová, and E. Streiblová. 1986. Immunofluorescence of the microtubular skeleton in growing and drug-treated yeast protoplasts. *Eur. J. Cell Biol.* 41:150–156.
21. Hiraoka, Y., T. Toda, and M. Yanagida. 1984. The *NDA3* gene of fission yeast encodes β-tubulin: a cold-sensitive *nda3* mutation reversibly blocks spindle formation and chromosome movement in mitosis. *Cell.* 39:349–358.
22. Hoebeke, J., G. Van Nijen, and M. De Brabander. 1976. Interaction of oncodazole (R 17934), a new antitumoral drug, with rat brain tubulin. *Biochem. Biophys. Res. Commun.* 69:319–324.

23. Howard, R. J. 1981. Ultrastructural analysis of hyphal tip cell growth in fungi: spitzenkorper, cytoskeleton and endomembranes after freeze-substitution. *J. Cell Sci.* 48:89–103.
24. Howard, R. J., and J. R. Aist. 1980. Cytoplasmic microtubules and fungal morphogenesis: ultrastructural effects of methyl benzimidazole-2-yl carbamate determined by freeze-substitution of hyphal tip cells. *J. Cell Biol.* 87:55–64.
25. Huffaker, T. C., J. H. Thomas, and D. Botstein. 1988. Diverse effects of β-tubulin mutations on microtubule formation and function. *J. Cell Biol.* 107:1997–2010.
26. Jacobs, C. W., A. E. M. Adams, and J. R. Pringle. 1984. Bud formation in yeast does not require cytoplasmic microtubules. *J. Cell Biol.* 99(No. 4, Pt. 2):43a. (Abstr.).
27. Jacobs, C. W., and P. J. Szaniszlo. 1982. Microtubule function and its relation to cellular development and the yeast cell cycle in *Wangiella dermatitidis*. *Arch. Microbiol.* 133:155–161.
28. Kilmartin, J. V. 1981. Purification of yeast tubulin by self-assembly *in vitro*. *Biochemistry.* 20:3629–3633.
29. Kilmartin, J. V., and A. E. M. Adams. 1984. Structural rearrangements of tubulin and actin during the cell cycle of the yeast *Saccharomyces*. *J. Cell Biol.* 98:922–933.
30. Kilmartin, J. V., and J. Fogg. 1982. Partial purification of yeast spindle pole bodies. *In* Microtubules in Microorganisms. P. Cappuccinelli and N. R. Morris, editors. Marcel Dekker, New York. 157–170.
31. Kilmartin, J. V., B. Wright, and C. Milstein. 1982. Rat monoclonal antitubulin antibodies derived by using a new nonsecreting rat cell line. *J. Cell Biol.* 93:576–582.
32. King, S. M., and J. S. Hyams. 1982. The mitotic spindle of *Saccharomyces cerevisiae*: assembly, structure and function. *Micron.* 13:93–117.
33. Lee, J. C., D. J. Field, and L. L. Y. Lee. 1980. Effects of nocodazole on structures of calf brain tubulin. *Biochemistry.* 19:6209–6215.
34. Leslie, R. J., and J. D. Pickett-Heaps. 1983. Ultraviolet microbeam irradiations of mitotic diatoms: investigation of spindle elongation. *J. Cell Biol.* 96:548–561.
35. Lillie, S. H., and J. R. Pringle. 1980. Reserve carbohydrate metabolism in *Saccharomyces cerevisiae*: responses to nutrient limitation. *J. Bacteriol.* 143:1384–1394.
36. Matile, P., H. Moor, and C. F. Robinow. 1969. Yeast cytology. *In* The Yeasts. Vol. 1. Biology of Yeasts. A. H. Rose and J. S. Harrison, editors. Academic Press, New York. 219–302.
37. McNiven, M. A., and K. R. Porter. 1986. Microtubule polarity confers direction to pigment transport in chromatophores. *J. Cell Biol.* 103: 1547–1555.
38. Mineyuki, Y., and M. Furuya. 1985. Involvement of microtubules on nuclear positioning during apical growth in *Adiantum* protonemata. *Plant Cell Physiol.* 26:627–634.
39. Moens, P. B., and E. Rapport. 1971. Spindles, spindle plaques, and meiosis in the yeast *Saccharomyces cerevisiae* (Hansen). *J. Cell Biol.* 50:344–361.
40. Neff, N. F., J. H. Thomas, P. Grisafi, and D. Botstein. 1983. Isolation of the beta-tubulin gene from yeast and demonstration of its essential function *in vivo*. *Cell.* 33:211–219.
41. Novick, P., and D. Botstein. 1985. Phenotypic analysis of temperature-sensitive yeast actin mutants. *Cell.* 40:405–416.
42. Oakley, B. R., and N. R. Morris. 1981. A β-tubulin mutation in *Aspergillus nidulans* that blocks microtubule function without blocking assembly. *Cell.* 24:837–845.
43. Oakley, B. R., and J. E. Rinehart. 1985. Mitochondria and nuclei move by different mechanisms in *Aspergillus nidulans*. *J. Cell Biol.* 101:2392–2397.
44. Osborn, M., R. E. Webster, and K. Weber. 1978. Individual microtubules viewed by immunofluorescence and electron microscopy in the same PtK2 cell. *J. Cell Biol.* 77:R27–R34.
45. Peterson, J. B., and H. Ris. 1976. Electron-microscopic study of the spindle and chromosome movement in the yeast *Saccharomyces cerevisiae*. *J. Cell Sci.* 22:219–242.
46. Pickett-Heaps, J., T. Spurck, and D. Tippit. 1984. Chromosome motion and the spindle matrix. *J. Cell Biol.* 99(Suppl.):137*s*–143*s*.
47. Pillus, L., and F. Solomon. 1986. Components of microtubular structures in *Saccharomyces cerevisiae*. *Proc. Natl. Acad. Sci. USA.* 83:2468–2472.
48. Pringle, J. R. 1978. The use of conditional lethal cell cycle mutants for temporal and functional sequence mapping of cell cycle events. *J. Cell. Physiol.* 95:393–406.
49. Pringle, J. R., and L. H. Hartwell. 1981. *Saccharomyces cerevisiae* cell cycle. *In* The Molecular Biology of the Yeast *Saccharomyces*. J. N. Strathern, E. W. Jones, and J. R. Broach, editors. Cold Spring Harbor Laboratory, Cold Spring Harbor, New York. 97–142.
50. Pringle, J. R., S. H. Lillie, A. E. M. Adams, C. W. Jacobs, B. K. Haarer, K. G. Coleman, J. S. Robinson, L. Bloom, and R. A. Preston. 1986. Cellular morphogenesis in the yeast cell cycle. *In* Yeast Cell Biology. J. Hicks, editor. Alan R. Liss, New York. 47–80.
51. Pringle, J. R., and J.-R. Mor. 1975. Methods for monitoring the growth of yeast cultures and for dealing with the clumping problem. *Meth. Cell Biol.* 11:131–168.
52. Quatrano, R. S., L. R. Griffing, V. Huber-Walchli, and R. S. Doubet. 1985. Cytological and biochemical requirements for the establishment of a polar cell. *J. Cell Sci.* 2(Suppl.):129–141.
53. Quinlan, R. A., C. I. Pogson, and K. Gull. 1980. The influence of the microtubule inhibitor, methyl benzimidazol-2-yl-carbamate (MBC) on nuclear division and the cell cycle in *Saccharomyces cerevisiae*. *J. Cell Sci.* 46:341–352.
54. Rindler, M. J., I. E. Ivanov, and D. D. Sabatini. 1987. Microtubule-acting drugs lead to the nonpolarized delivery of the influenza hemagglutinin to the cell surface of polarized Madin-Darby canine kidney cells. *J. Cell Biol.* 104:231–241.
55. Robinow, C. F., and J. Marak. 1966. A fiber apparatus in the nucleus of the yeast cell. *J. Cell Biol.* 29:129–151.
56. Rogalski, A. A., J. E. Bergmann, and S. J. Singer. 1984. Effect of microtubule assembly status on the intracellular processing and surface expression of an integral protein of the plasma membrane. *J. Cell Biol.* 99: 1101–1109.
57. Rose, M. D., and G. R. Fink. 1987. *KAR1*, a gene required for function of both intranuclear and extranuclear microtubules in yeast. *Cell.* 48: 1047–1060.
58. Schatz, P. J., L. Pillus, P. Grisafi, F. Solomon, and D. Botstein. 1986. Two functional α-tubulin genes of the yeast *Saccharomyces cerevisiae* encode divergent proteins. *Mol. Cell. Biol.* 6:3711–3721.
59. Schatz, P. J., F. Solomon, and D. Botstein. 1986. Genetically essential and nonessential α-tubulin genes specify functionally interchangeable proteins. *Mol. Cell. Biol.* 6:3722–3733.
60. Schekman, R. 1985. Protein localization and membrane traffic in yeast. *Annu. Rev. Cell Biol.* 1:115–143.
61. Schliwa, M. 1984. Mechanisms of intracellular organelle transport. *In* Cell and Muscle Motility. 5. The Cytoskeleton. J. W. Shay, editor. Plenum Press, New York. 1–82.
62. Schulze, E., and M. Kirschner. 1987. Dynamic and stable populations of microtubules in cells. *J. Cell Biol.* 104:277–288.
63. Sheetz, M. P., and J. A. Spudich. 1983. Movement of myosin-coated fluorescent beads on actin cables *in vitro*. *Nature (Lond.).* 303:31–35.
64. Sloat, B. F., A. E. M. Adams, and J. R. Pringle. 1981. Roles of the *CDC24* gene product in cellular morphogenesis during the *Saccharomyces cerevisiae* cell cycle. *J. Cell Biol.* 89:395–405.
65. Sloat, B. F., and J. R. Pringle. 1978. A mutant of yeast defective in cellular morphogenesis. *Science (Wash. DC).* 200:1171–1173.
66. Thomas, J. H., N. F. Neff, and D. Botstein. 1985. Isolation and characterization of mutations in the β-tubulin gene of *Saccharomyces cerevisiae*. *Genetics.* 112:715–734.
67. Tkacz, J. S., and J. O. Lampen. 1972. Wall replication in *Saccharomyces* species: use of fluorescein-conjugated concanavalin A to reveal the site of mannan insertion. *J. Gen. Microbiol.* 72:243–247.
68. Toda, T., Y. Adachi, Y. Hiraoka, and M. Yanagida. 1984. Identification of the pleiotropic cell division cycle gene *NDA2* as one of two different α-tubulin genes in *Schizosaccharomyces pombe*. *Cell.* 37:233–242.
69. Toda, T., K. Umesono, A. Hirata, and M. Yanagida. 1983. Cold-sensitive nuclear division arrest mutants of the fission yeast *Schizosaccharomyces pombe*. *J. Mol. Biol.* 168:251–270.
70. Umesono, K., T. Toda, S. Hayashi, and M. Yanagida. 1983. Two cell division cycle genes *NDA2* and *NDA3* of the fission yeast *Schizosaccharomyces pombe* control microtubular organization and sensitivity to anti-mitotic benzimidazole compounds. *J. Mol. Biol.* 168:271–284.
71. Vale, R. D., J. M. Scholey, and M. P. Sheetz. 1986. Kinesin: possible biological roles for a new microtubule motor. *Trends Biochem. Sci.* 11: 464–468.
72. Watts, F. Z., D. M. Miller, and E. Orr. 1985. Identification of myosin heavy chain in *Saccharomyces cerevisiae*. *Nature (Lond.).* 316:83–85.
73. Wilkinson, L. E., and J. R. Pringle. 1974. Transient G1 arrest of *Saccharomyces cerevisiae* cells of mating type alpha by a factor produced by cells of mating type *a*. *Exp. Cell Res.* 89:174–187.
74. Williamson, D. H., and D. J. Fennell. 1975. The use of fluorescent DNA-binding agent for detecting and separating yeast mitochondrial DNA. *Meth. Cell Biol.* 12:335–351.
75. Wood, J. S. 1982. Genetic effects of methyl benzimidazole-2-yl-carbamate on *Saccharomyces cerevisiae*. *Mol. Cell. Biol.* 2:1064–1079.
76. Wood, J. S., and L. H. Hartwell. 1982. A dependent pathway of gene functions leading to chromosome segregation in *Saccharomyces cerevisiae*. *J. Cell Biol.* 94:718–726.